3 Systems, Model and Technical Details

3.1 General Consideration

We study **interface properties** of two different types of systems; (1) the first type of systems consist of interfaces between polymers of different stiffnesses which is called **'stiffness disparity'**, and (2) the second one consist of interfaces between polymers having different sizes of monomers which is called **'monomer size disparity'**. In the first case, apart from interface properties, the **phase-behavior** of polymer blends with **low stiffness disparity** also has been studied. The models for these two types of systems are different and described in section 3.2 and 3.3 respectively. To study interface properties and phase separation for the systems outlined above, a numerical code based on **coarse grained continuous-space (off-lattice)** model, has been developed. Our approach differs significantly from the previous numerical studies which use lattice models almost exclusively [42]. For the systems with interfaces continuous space (CS) model serves better than the lattice model. Besides their inherent spatial isotropy and the absence of pinning the CS models offer a simple way to determine surface tension by measuring the pressure tensor which is one of the main goals of this work. Off-lattice polymer constructions [7, 42, 46], in which varying angles and free rotation about the covalent bonds are permitted, which is not possible due to restricted geometry in lattice models, is a more general way than the lattice models to create the semiflexible chains of any stiffness. Further provided the forces are short ranged, theoretical work [72] suggests that interfaces in the continuum exhibit no roughening transition. Moreover, lattice model is not a suitable choice to study monomer size disparity system.

The coarse-grained model can be obtained by combining n successive covalent bonds along the backbone of a polymer chain into one effective segment. The coarse-graining is done in such a way that the large-scale geometrical structure of the polymer coil is left invariant, e.g; properties such as radius of gyration of the coil and the probability distribution of its end-to-end distance are the same for the coarse-grained model and for the chemically detailed model. This invariance of long wavelength properties can be realized by introducing suitable potentials in the coarse grained model which control bond lengths of the effective bonds, angles between effective bonds along the sequence of the coarse-grained chain etc.. In coarse grained models, one loses the relevant information

on a very small length scale only [42]. Coarse grained models which retain a minimal set of relevant polymeric properties like, the connectivity of the macromolecules along the bakbone, the excluded volume of the beads, and short ranged thermal interactions have proven extremely efficient in investigating the universal thermodynamic properties of polymeric multicomponent systems. Simulations performed on this coarse-grained level require only a small number of parameters to compare with experiments and analytical theory quantitatively [4].

Coarse grainning can be done in both lattice model and in off-lattice model. There is no unique model description of a polymer chain system; infact, for different physical questions somewhat different models are optimal. For example, constant pressure simulations of lattice models are difficult, whereas their implementation is relatively straight forward for off-lattice models. Even at constant volume, off-lattice models have the advantage that the pressure and the interfacial tension can be measured via the virial theorem [7, 73, 74]. Moreover, off-lattice models are useful to capture hydrodynamic flow in molecular dynamics simulations because by construction coarse grained CS model keeps the long wavelength properties invarient. At the same time, off-lattice models are more demanding with respect to computational resources while model like bond fluctuation and other lattice models are well suited to the study of polymer melt dynamics, the glass transition etc. [42].

3.2 Model for Stiffness Disparity

3.2.1 Model

We performed computer simulations of the interface properties of a three dimensional phase separated sandwich-type system of flexible and semiflexible polymers. Figure 3.1 shows a typical snapshot of such a system.

As chain models a coarse grained continuous space model has been used. This off-lattice model provides a more direct way, by setting restriction on bond angles, to generate the semiflexible chains and allows the investigation of chains of any stiffness. The polymer chains are modeled using the rod-bead model [42, 7] by a succession of jointed spherical monomers. Each chain consists of N (with N =32) spheres of equal diameter $d_{min} = \sqrt{3}$ which are connected by (N-1) bonds of variable length $d_{min} \leq d \leq d_{max} \approx \frac{4}{3} d_{min}$. In our model the excluded volume is taken into account by the following potential, $V_{ex}(r)$, between any two beads separated by a distance r;

$$V_{ex}(r) = \begin{cases} 0 & , \text{ if } r > d_{min} \text{ (diameter of the monomers)} \\ \infty & , \text{ else.} \end{cases} \tag{3.1}$$

This excluded volume potential between any two beads is shown in the figure 3.2.

Similarly, the connectivity of chains is taken into account by following potential, $V_{con}(r)$, between any two consecutive beads of a chain at a distance r;

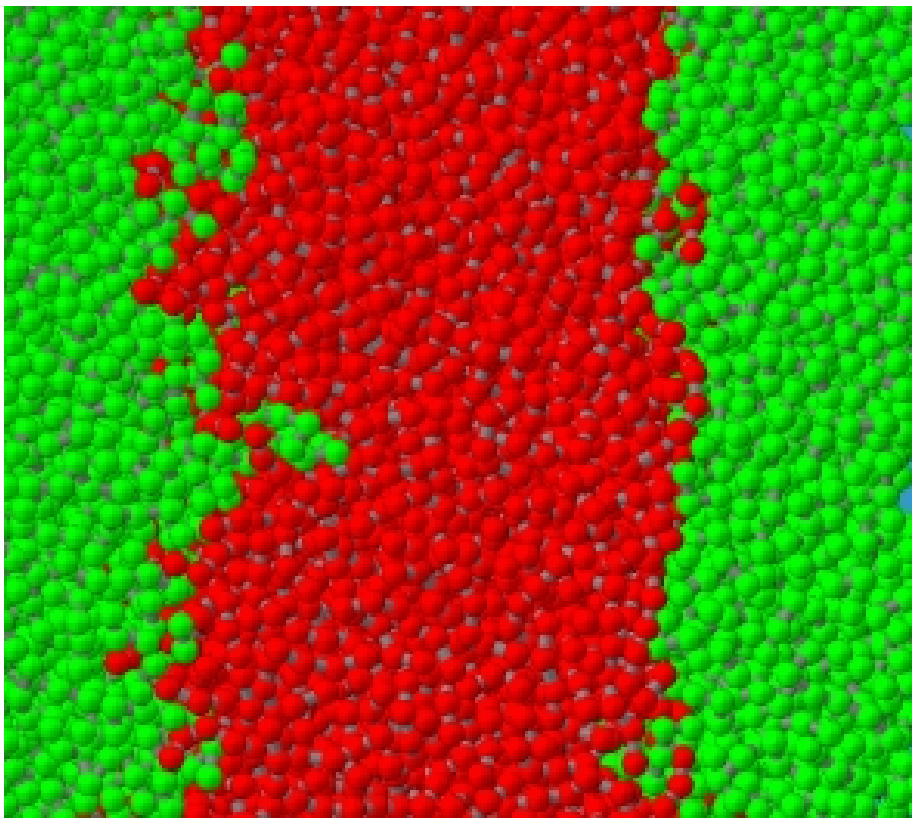

Figure 3.1: A typical system of study in which green monomers are from flexible chains and red from semiflexible chains whose flexibility varies from flexible to almost stiff rod.

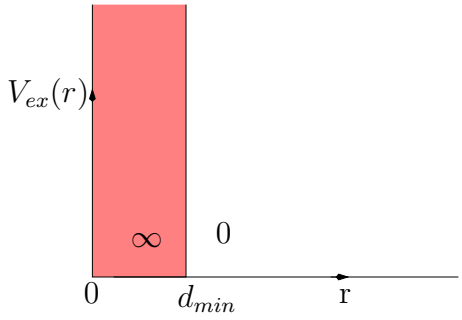

Figure 3.2: Excluded volume potential between any two beads separated by a distance r in stiffness disparity system.

$$V_{con}(r) = \begin{cases} 0 & , \text{ if } d_{min} \leq r \leq d_{max} \\ \infty & , \text{ else} \end{cases} \tag{3.2}$$

where d_{min} and d_{max} are already defined. The potential of connectivity $V_{con}(r)$, between

two successive beads of a chain is shown in the figure 3.3. In the same way as in ex-

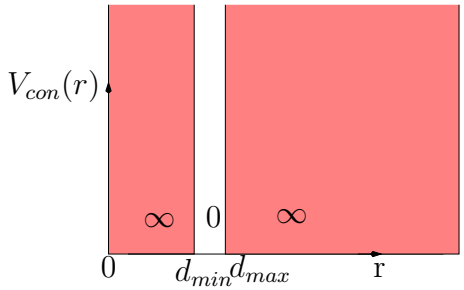

Figure 3.3: connectivity potential between two consecutive beads of a polyme chain.

cluded volume and connectivity, the potential for the bending restrictions (in semiflexible chains) also is a stepwise potential see figure 3.4. Therefore, the bending restrictions is defined by the following potential;

$$V_{bending}(\theta) = \begin{cases} 0 & , \text{ if } \theta < \theta_{max} \\ \infty & , \text{ else} \end{cases}$$

where θ is the angle between any two consecutive bond vectors of a semiflexible chain (see figure 3.5) and θ_{max} is maximum angle between two consecutive bond vectors of a semiflexible chain permitted in the system. Choosing different values of θ_{max} we can generate semiflexible chains of any stiffness, ranging from flexible to stiff rod.

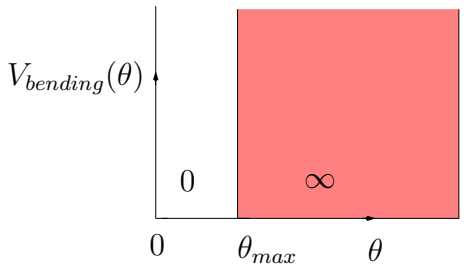

Figure 3.4: Bending potential for a semiflexible chain. θ is the angle between any two consecutive bond vectors of the chain.

Semiflexible chains in which the angle between two consecutive bond vectors (θ in Figure 3.5) is not larger than 90°, 75°, 60°, 45°, 30°, 15° and 5° (the stiffest case studied which is refered through out the present work as almost stiff rod) are generated. The whole system consists of 512 flexible and semiflexible chains respective.

The interaction between segments which are not jointed directly is also modeled by a stepwise potential. For simplicity, we assume that the interaction between equal

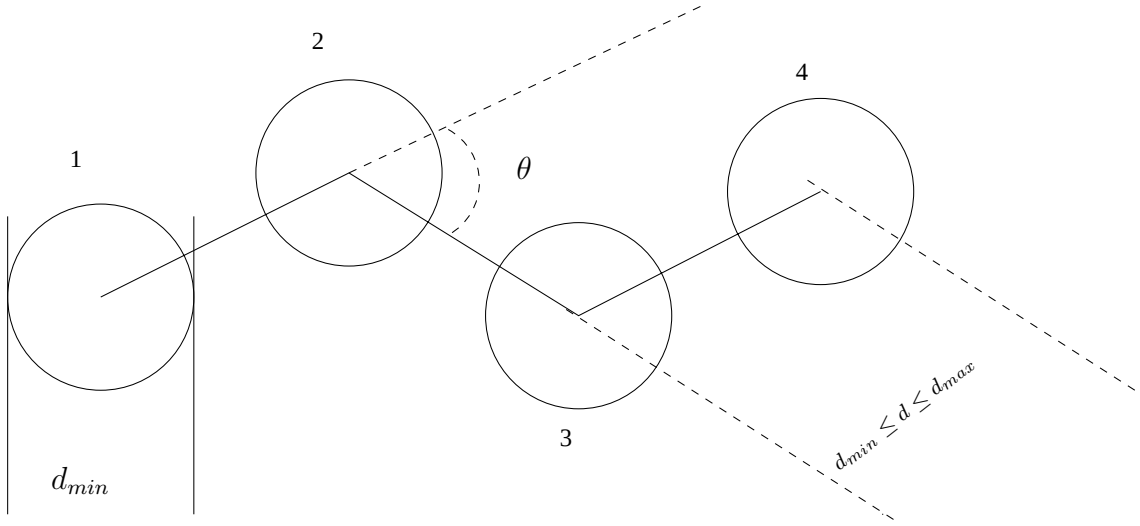

Figure 3.5: Semiflexible chain model. $\theta \leq \theta_{max}$, the maximum angle chosen between two consecutive bond vectors.

types of monomers A and B (type A for flexible chains and type B for semiflexible chains), $V_{AA} = V_{BB} = 0$ and a repulsive potential acts between different monomers $V_{AB} = k_B T\varepsilon$ where k_B is Boltzmann constant and T is temperature and ϵ is the repulsive interaction parameter between different types of beads and $\epsilon = 0.1$ to study the interface properties in strong segregation limit. However, to study phase behavior using the interface properties of weak segregation limit the value of ϵ is decreased. Therefore, ϵ is related to the Flory-Huggins parameter, χ, [12] in this model (see below). The interaction potential is depicted in figure 3.6. The assumed range of the interaction between two different types of monomers is denoted by d_{2type}, in the present work, and it has value $\sim \sqrt{\frac{5}{3}} d_{min}$. This interaction potential between any two different types of monomers can be expressed by following equation;

$$V_{AB}(r) = \begin{cases} k_B T\epsilon & , \text{ if } d_{min} < r < d_{2type} \\ \infty & , \text{ if } r < d_{min} \\ 0 & , \text{ if } r > d_{2type} \end{cases}$$

where $V_{AB}(r)$ is the interaction potential between monomers of type A and type B separated by a distance r. This potential is shown in the figure 3.6.

For estimations of the Flory-Huggins parameter the average number of interchain contacts z_{eff} of a monomer within a sphere of radius of the interaction range is determined for the pure components. The Flory-Huggins parameter

$$\chi = \frac{z_{eff,flex} + z_{eff,stiff}}{2} \cdot \varepsilon \tag{3.3}$$

increases slightly with increasing stiffness of the semiflexible component because in the semiflexible chains the contacts of monomers from other chains increase. For the flexible

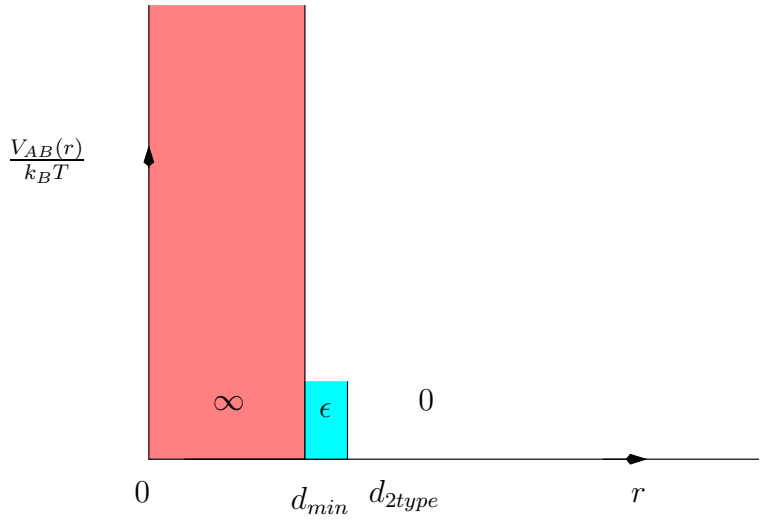

Figure 3.6: Interaction potential between two different types of beads at a distance r.

chains χ is 0.32 and it is 0.366 for the stiffest case studied for $\epsilon = 0.1$ (see above). The value of $N\chi$ is much higher than two and therefore our results correspond to strongly immiscible blends and a stable interface can be expected for $\epsilon = 0.1$.

3.2.2 Generation of Chains and Equilibration

To generate a system of stiffness disparity, 32 random walk chains (flexible chains) with random bond length distribution $d_{min} \leq d \leq d_{max}$ with no overlap with next nearest neighbors within the chain [7] are generated. Other 32 random walk chains (semiflexible chains) are generated by setting additional constraint on the bond angles between two consecutive bond vectors of a chain viz; $0 \leq \theta \leq \theta_{max}$ where θ is angle between two consecutive bond vectors of a chain and θ_{max} is the maximum angle between two consecutive bond vectors of a chain chosen in the system of study. To generate the interface initially we have considered the initial box having three compartments in which the middle one has volume double than that of both sides (this simulation box has dimensions $64 \times 16 \times 16$). One fourth of both sides of the box (along x-dimension) occupy flexible chains and the remaining half of the box in the middle with semiflexible chains randomly. Therefore, there are two interfaces located at $\frac{1}{4}$th and $\frac{3}{4}$th of the x-dimension of the box. The overlaps between the segments are removed by stepwise increase ("blowing up") of the diameter of the spherical monomers followed by Monte Carlo steps. This process is started with the minimum distance of any non directly connected monomers and repeated until the minimum distance between any two monomers is equal or greater than d_{min}. After removing the overlaps the size of the system is doubled by shifting y and z coordinates to get a system of 256 chains in a $64 \times 32 \times 32$ - parallelepiped. We further multiply the system by shifting y and z coordinates to get finally the system

of study with 1024 chains in a $64 \times 64 \times 64$ - cube. Figure 3.7 shows one of such a system which contains flexible chains and semiflexible chains with $\frac{l_p}{a}$ =2 where l_p is the persistence length (see page 27) and a is the average bond length (see below).

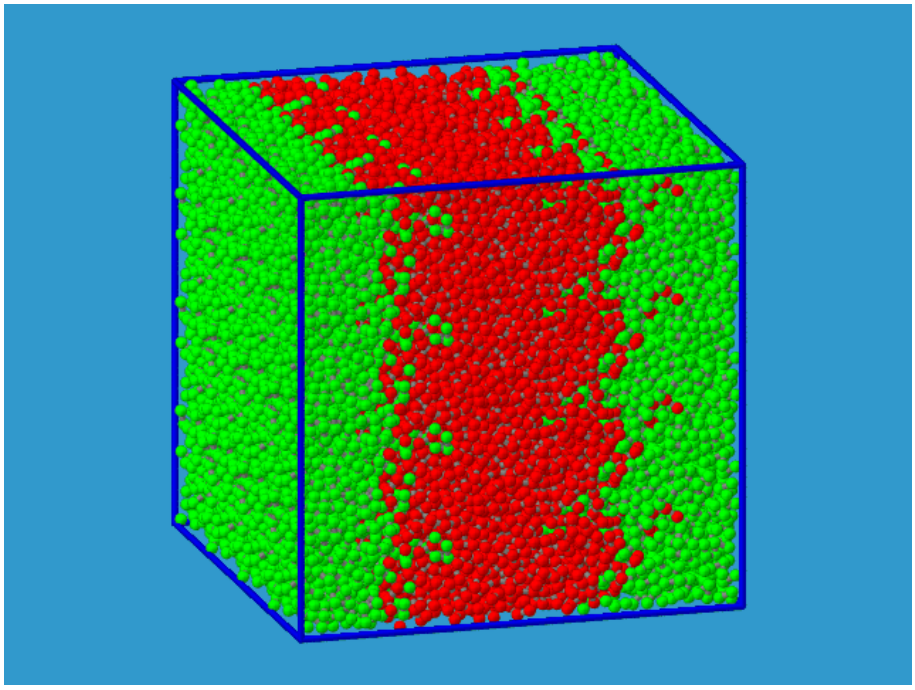

Figure 3.7: Initial configuration for a system with flexible chains and semiflexible chains of persistence length $(\frac{l_p}{a})$= 2.

Since the systems of study considers also very high stiff chains which form a nematic phase, such a very stiff chains are generated in a different way than described above. We tried to get equilibrium configuration for systems in which persistence length $(\frac{l_p}{a})$ of the semiflexible chain is greater than 13.6 following the method described above. However, the system containing highly stiff chains form several domains (within a domain the chains allign parallel to each other) and we could not get monodomain phase separated equilibrium system. Therefore, to generate a system with highly stiff chains, persistence length greater than 13.6, and flexible chains, we follow the method described below. First, 512 stiff chains each chain containing 32 monomers are generated. All the chains allign parallel to $Z - axis$ of the simulation box and occupy middle half portion of the box having dimensions $64 \times 64 \times 64$. We performed random movement of the stiff chains (along Z-axis) such that the mean squared displacement (MSD) of the center of mass of chains is a few times of R^2, mean squared end to end distance. The flexible chains which were already equilibrated occupy either side of the box whose center of mass is fixed to the $\frac{1}{4}$th of both sides of the box. The number of flexible chains is 512. After having the system of flexible-stiff chains the overlapping between any two monomers is checked. The diameter of both types of monomers is d_{min}. Then Monte-Carlo moves

were performed as described below for both types of the monomers with suitable angular restriction between two consecutive bond vectors of a stiff chain.

The interfacial properties of flexible polymers and liquid-crystalline polymers [9] depend upon the direction of nematic director (for example, see [75] for macromolecular systems and [76] for small molecular systems for the dependence of interfacial properties on direction of nematic director in isotropic-nematic interface). In the present study the most stable case in which nematic director is parallel to the interface plane will be considered.

For equilibration and thermodynamical averaging, we perform Monte-Carlo steps according the standard Metropolis algorithm with random choice of a monomer and cyclic choice of one of the six directions along the coordinate axes (see the flow diagram). A move is accepted according to transition probability $P(E) = \mathrm{Min}(1,\exp(-\frac{\delta E}{k_B T})) > \zeta$ where δE is difference of energy of new and old configurations, k_B is Boltzmann constant, T is temperature and $1 > \zeta > 0$ is a random number. The length of an attempted step between zero and a maximum step length $\sim\ 0.23 \times d_{min}$ is chosen randomly. To accelerate the tests for hard-core overlapping and the calculations of the interaction energy after each attempted move, we follow the standard way by dividing the simulation box into cubic cells of size l_c with single occupancy and checking the particles in the neighborhood of the moved particle only. Single occupancy is realized by the choice $d_{min} = \sqrt{3} \times l_c$. The details of the linked cell method are described in [77, 78]. Further Auhl [7] has applied the linked cell method for the flexible-flexible polymer systems. However, for semiflexible chains we have to check angle between two consecutive bond vectors of the chain (see the flow diagram). Two well defined interfaces are enforced in the canonical ensemble in a thick film geometry ($L \times L \times L$), with periodic boundary conditions in all the three directions. The interfaces are on average located in $\frac{1}{4}$th and $\frac{3}{4}$th of the x-dimensions of the simulation box. A Monte Carlo step for a monomer from flexible chain and a monomer from semiflexible chain are described in the flow diagram, figures 3.8 and 3.9.

To know whether a system has attained equilibrium configuration, the following criterion is used. The parallel and the perpendicular (parallel and perpendicular according to the interface) components of the radius of gyration R_g and the displacement of center of mass of chains against the simulation time are monitored. According to this criterion, system with interfaces will be expected in equilibrium when the mean squared displacement (ΔMSD) of center of mass of chains, after removal of overlaps between monomers, is comparable to the mean squared radius of gyration of chains, R_g^2. The figure 3.10 presents mean squared displacement of center of mass of chains and mean squared parallel and perpendicular components of radius of gyration for the system with chains having persistence length ($\frac{l_p}{a}$)= 2.0 and flexible chains. For each system of study, the ΔMSD of center of mass of chains and parallel and perpendicular components of R_g^2 are monitored. If both of theses quantities are comparable, calculations of interfacial tensions and other quantities (see below) are started. Further, the ΔMSD of individ-

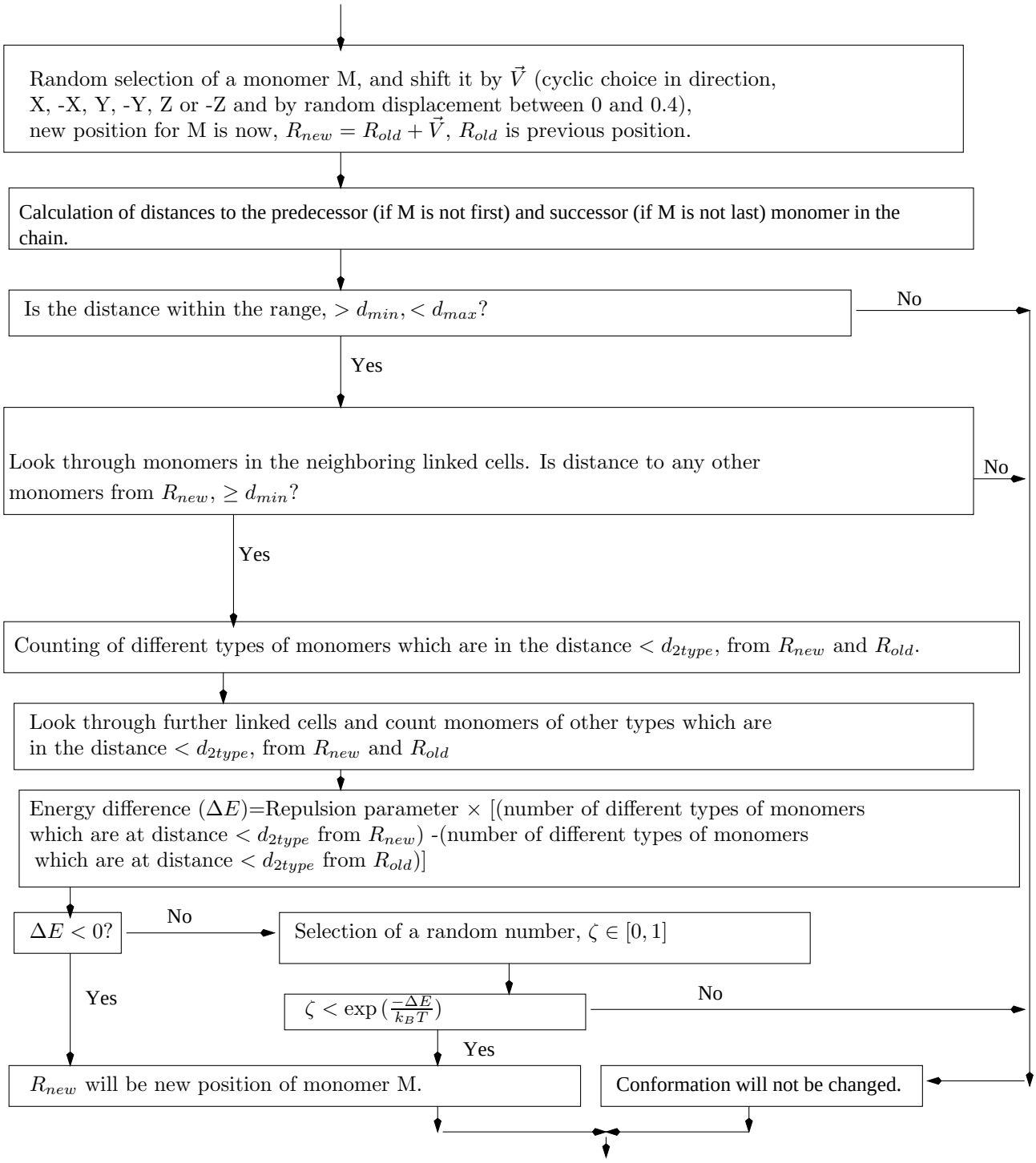

Figure 3.8: Flow diagram for a monomer from flexible chains.

ual components (flexible and semiflexible) also are not significantly different than that of the sum of both components. To get equilibrium state 6.1×10^5 attempted moves

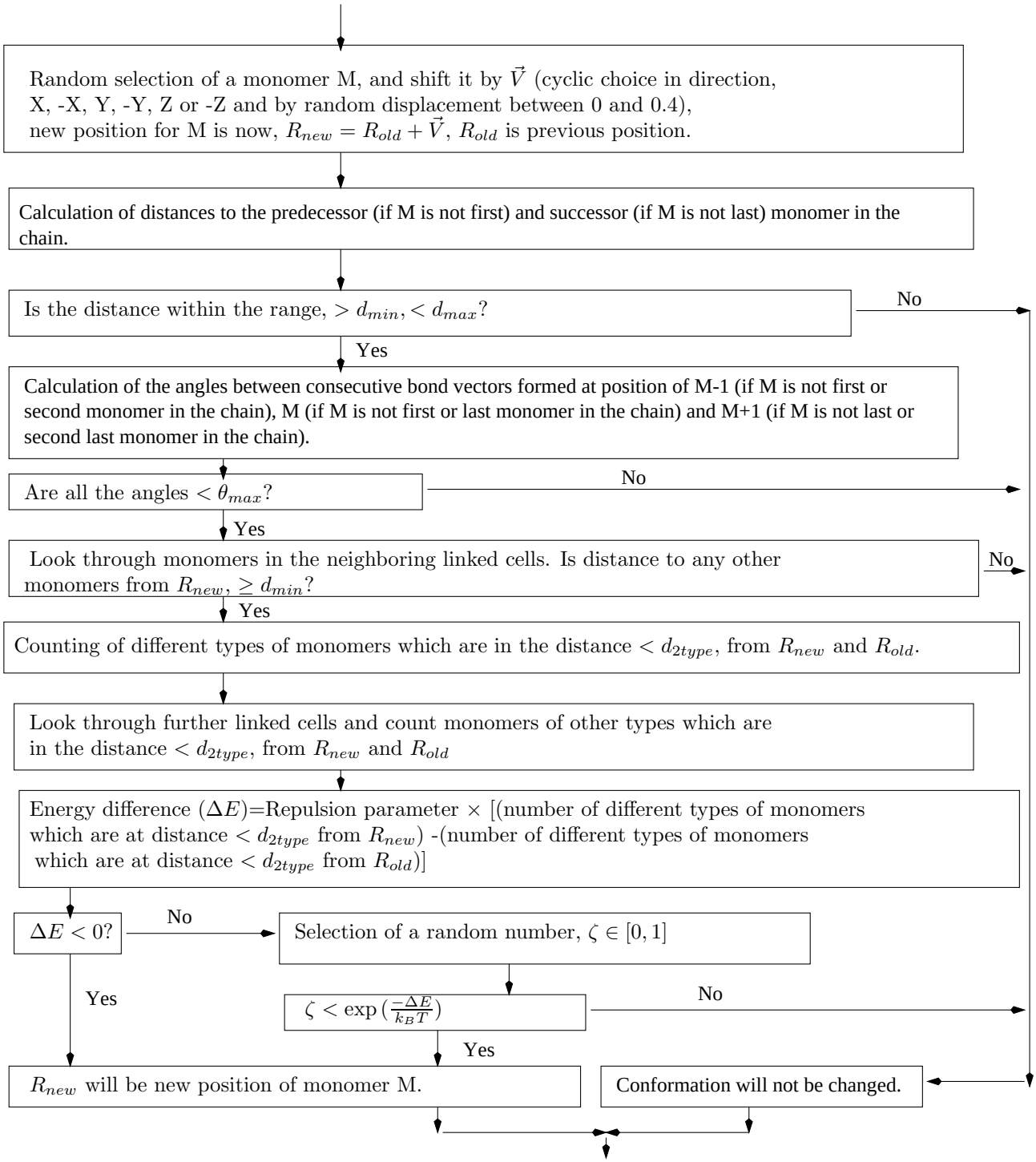

Figure 3.9: Flow diagram for monomers from semiflexible chains.

per monomer (AMM) were performed for the system with flexible chains. The AMM increase with the stiffness of the semiflexible components of the system and 6.1×10^7

AMM were performed for the system which contains flexible chains and chains with persistence length ($\frac{l_p}{a}$)= 13.6. For an isotropic-nematic interface also 6.1×10^7 AMM were performed by keeping the proper restriction on the angle between two consecutive bond vectors of a chain. To be ensured that the system is close enough to equilibrium, the values of interfacial tensions are monitored during the calculations. The values of interfacial tensions of the system, in which semiflexible component has persistence length ($\frac{l_p}{a}$)= 2.5, against number of calculations are depicted in figure 3.12. They also show that (as the values do not decrease monotonically with the time of calculations) the systems are close enough to equilibrium at the time of calculation. Figure 3.11 shows one typical configuration after achieving equilibrium condition.

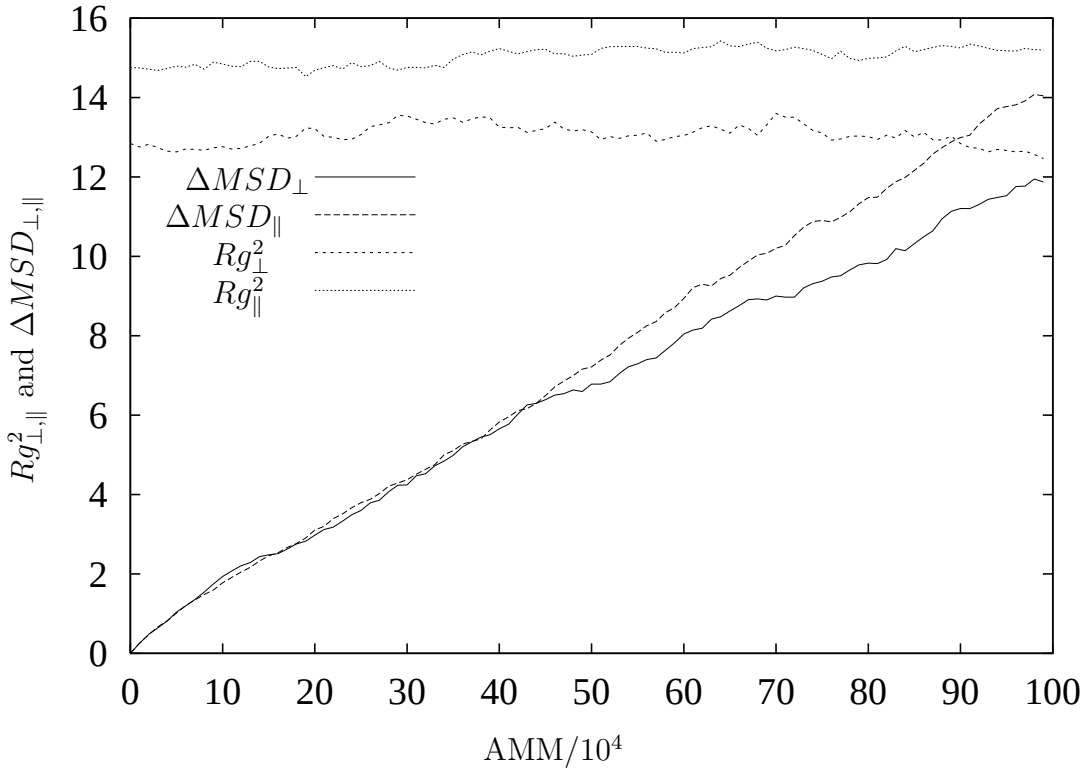

Figure 3.10: Mean squared displacement of center of mass and parallel and perpendicualr components of radius of gyration during the Monte Carlo steps for a system containing flexible chains and semiflexible chains with persistence length ($\frac{l_p}{a}$)=2.

3.2.3 Single Chain Properties and Nematic Order Parameter

After describing the methods to generate the chains and attain the equilibrium configuration in subsection 3.2.2, the single chain properties and ordering of the highly stiff chains will be described in this subsection.

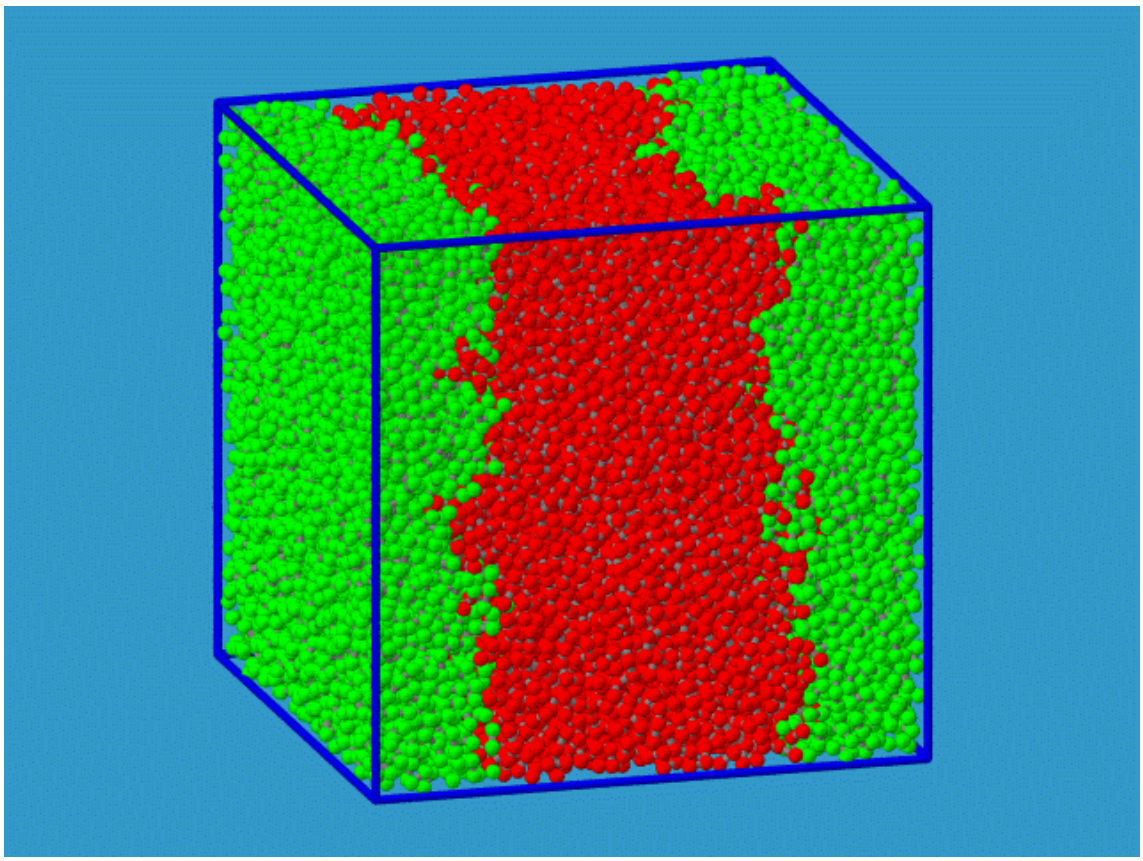

Figure 3.11: Equilibrated configuration for a system with flexible chains and semiflexible chains with persistence length ($\frac{l_p}{a}$)= 2.

Single chain properties

Before going over to present the results, we first define the quantities which characterize the single chain properties by the help of figure 3.13. The end to end vector is denoted by $\vec{R}$ and the mean squared end to end distance is, R^2. Similarly, R_g^2 is the mean squared radius of gyration and $R_g^2(0)$ is the mean squared radius of gyration of the flexible chains. The lower bound of statistical segment length, b, is introduced in the following way;

$$b = \frac{R^2}{L} = aC_{1N} \tag{3.4}$$

where $L = Na$ is contour length, a is the average bond length and C_{1N} is ratio of R^2 and Na^2 which is denoted by C_∞ in literatures when $N \to \infty$. The aspect ratio Γ is defined as the ratio of statistical segment length b and diameter of the bead d_{min} i.e. $\Gamma = \frac{b}{d_{min}}$. The persistence length, l_p, is calculated by the average of projection of end to end vector along the unit vector in the direction of first bond. Therefore, l_p is calculated using the following formula [79];

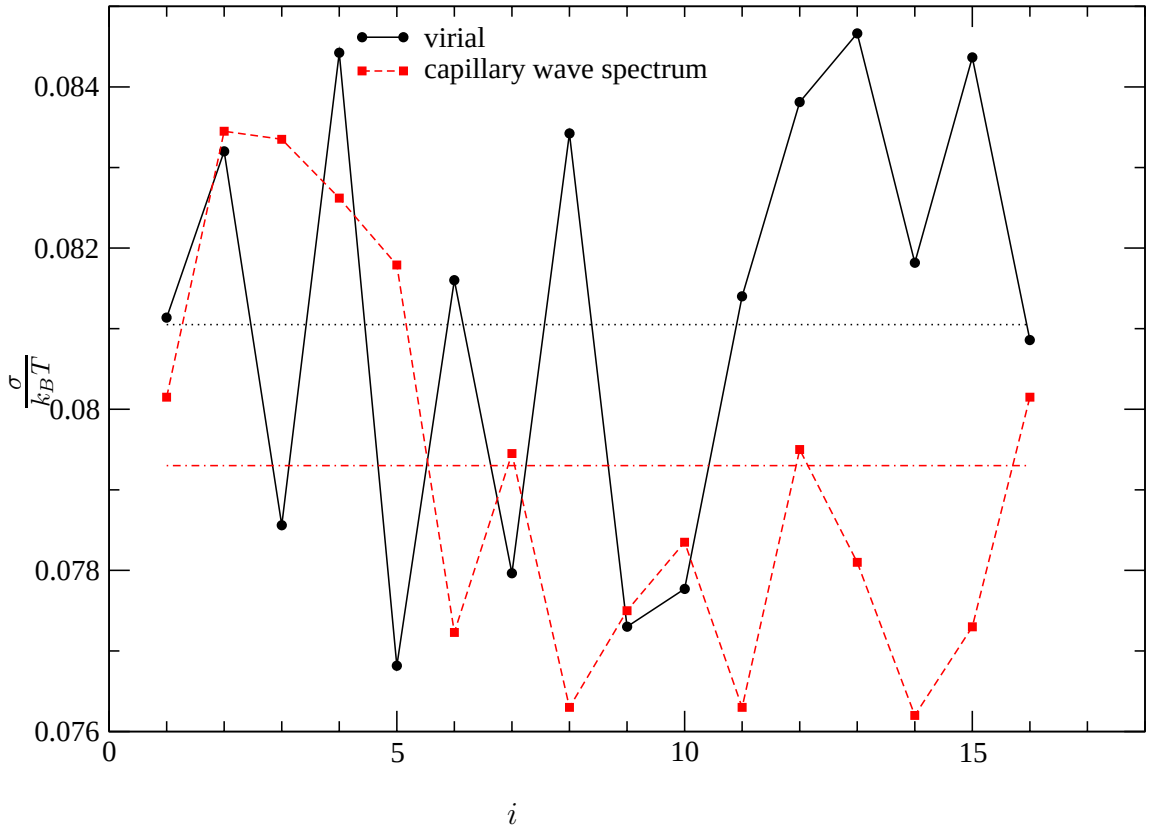

Figure 3.12: Interfacial tension as a function of number of calculations for a system with flexible chains and semiflexible chains with persistence length ($\frac{l_p}{a}$)= 2.5. There are 3.4×10^4 AMM between two succesive calculations.

$$l_p = \left\langle \vec{R} \cdot \vec{u}_1 \right\rangle = \frac{1}{a} \sum_{i=0}^{N} \langle \vec{a}_1 \cdot \vec{a}_i \rangle \tag{3.5}$$

where a is the average bond length, $\vec{a}_i$ are ith bond vectors, $\vec{R}$ are the end to end vectors, $\vec{u}_1 = \frac{\vec{a}_1}{a}$ are the unit vectors along first bond vector and N is the number of monomers in a chain. l_p and/or C_{1N} defines the chain stiffness.

Figure 3.13 shows the projection of end to end vector along the first bond vector. In table 3.1, single chain conformational properties as a function of stiffness of semiflexible component for all the systems are discussed.

Nematic Order Parameter

To know whether the system is in nematic phase for highly stiff chains, the nematic order parameter has been calculated. To calculate nematic order parameter we need to know the nematic director. For stiff rod, it is very easy to find the nematic director

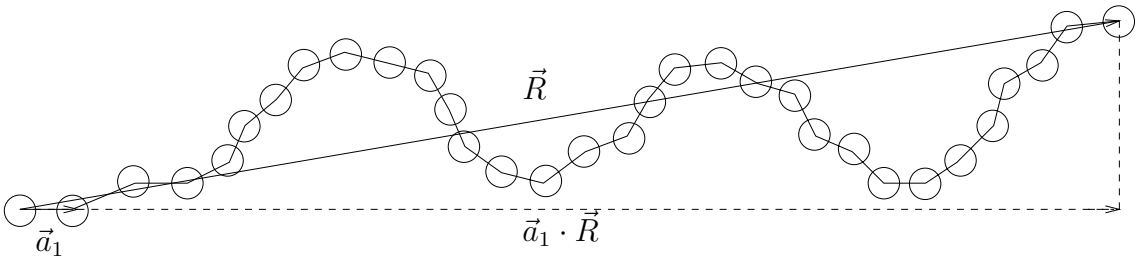

Figure 3.13: Projection of end to end vector ($\vec{R}$) along first bond vector in a semiflexible chain.

Flexibility	R^2	R_g^2	$\frac{R^2}{R_g^2}$	$\frac{b}{a}$	$\Gamma = \frac{b}{d_{min}}$	$\frac{l_p}{a}$	χ	S
Flexible	193	32	6.03	1.51	1.74	1.25	0.32	0.0082
90°	356	55	6.47	2.8	3.23	2	0.327	0.01
75°	511	76	6.72	4.03	4.65	2.5	0.335	0.0215
60°	766	106	7.22	6.07	7.00	4.2	0.340	0.053
45°	1309	159	8.23	10.4	12.00	7.2	0.346	0.097
30°	2217	220	10.07	17.6	20.32	13.6	0.351	0.16
15°	3657	327	11.18	28.91	33.38	28.0	0.362	0.97
5°	3801	339	11.21	30.05	34.69	30.02	0.366	0.99

Table 3.1: single chain conformations as a function of the stiffness parameter, here the persistence length ($\frac{l_p}{a}$) and statistical segment length ($\frac{b}{a}$) are in unit of bond length and S is the nematic order parameter described in the text. All these quantities discussed in this table increase as a function of stiffness.

however for semiflexible chains first we have to calculate the ordering tensor ($\mathbf{Q}$), for the chain ordering, by the following way [80]. The shape of the molecule is obtained by representing each chain in terms of semi-axis lengths of an equivalent spheroid with the same moment of inertia as the molecule and one can obtain this by diagonalizing the moment of inertia tensor of the molecule. For molecule 'k', the elements of the moment of inertia tensor, $\mathbf{I}_k$, are given by,

$$I_{\alpha\beta,k} = \sum_{i=1}^{N} (r_i^2 \delta_{\alpha\beta} - r_{i\alpha} r_{i\beta}) \tag{3.6}$$

where $\alpha, \beta = x,\ y,\ z$ are the cartesian coordinates, $\delta_{\alpha,\beta}$ is the Kronecker delta, $r_{i\alpha}$ is the distance in the α direction of site i from the center of mass of the molecule, and $r_i^2 = r_x^2 + r_y^2 + r_z^2$ and N is the number of monomer in the molecule 'k'. The eigenvector which is denoted by $\vec{e}_k$ corresponding to the smallest eigenvalue of $I_{\alpha\beta,k}$ is reffered to as the molecular axis vector of the chain. The nematic director for the semiflexible chains is obtained by diagonalizing the ordering tensor, $\mathbf{Q}$ defined by,

$$\mathbf{Q}_{\alpha\beta} = \frac{1}{N_p} \sum_{k=1}^{N_p} \frac{3}{2} e_{k\alpha} e_{k\beta} - \frac{1}{2} \delta_{\alpha\beta} \tag{3.7}$$

$e_{k\alpha}$ is the αth ($\alpha = x,\ y$ or z) component of the molecular axis vector, $\vec{e}_k$. Then the order parameter is given by,

$$S = -2 < \lambda > \tag{3.8}$$

where λ is the middle eigenvalue of $\mathbf{Q}$.

The nematic order parameters for the semiflexible component of the systems of study are presented in table 3.1. From table it is clear that upto persistence length $(\frac{l_p}{a}) = 13.6$ there is not nematic ordering but for higher values of persistence length the semiflexible polymers form the nematic phase.

Orientational parameters

Of special interest in a system containing stiff chains is the orientational order. In polymer systems, one can define orientational parameters in different length scales e.g. orientational parameter of bond vectors and chain orientational parameters. Systems with the planar interface in the $y - z-$plane has a distinguished direction along the $x-$axis, hence the order-parameter-field of bond ordering,

$$S\left(x\right) = \frac{3\left\langle a_x^2\left(x\right)\right\rangle - a^2}{2a^2} \tag{3.9}$$

is the most direct measure of the order near the interface and also in the bulk. $\langle a_x^2\left(x\right)\rangle$ and $\langle a^2\rangle$ are the mean squared of $x-$component of bond vector and of the bond vector respectively (see chapter 4).

In similar way, the chain orientational parameters, perpendicular ($\Delta Rg_\perp$) and parallel ($\Delta Rg_\parallel$), with respect to interface plane of chain orientation

$$\Delta Rg_\perp = \frac{3\left\langle Rg_x^2\right\rangle - \left\langle Rg^2\right\rangle}{\left\langle 2Rg^2\right\rangle} \tag{3.10}$$

and

$$\Delta Rg_\parallel = \frac{3(\left\langle Rg_z^2\right\rangle + \left\langle Rg_y^2\right\rangle)/2 - \left\langle Rg\right\rangle^2}{2\left\langle Rg^2\right\rangle} \tag{3.11}$$

can be introduced where $\langle Rg^2\rangle$ is the averaged radius of gyration of the chains and $\langle Rg_i^2\rangle$ $(i = x, y, z)$ is the corresponding component of square of radius of gyration of the polymer chains. Therefore, when the chains orient parallel to the interface, parallel orientational parameter $\Delta Rg_\parallel$ will be positive and has maximum value 0.25 while the perpendicular orientational parameter $\Delta Rg_\perp$ will be negative and has minimum value -0.5. Similarly, when the chains orient perpendicular to the interface, parallel orientational parameter $\Delta Rg_\parallel$ will be negative while the perpendicular orientational parameter $Rg_\perp$ will be positive (see chapter 4).

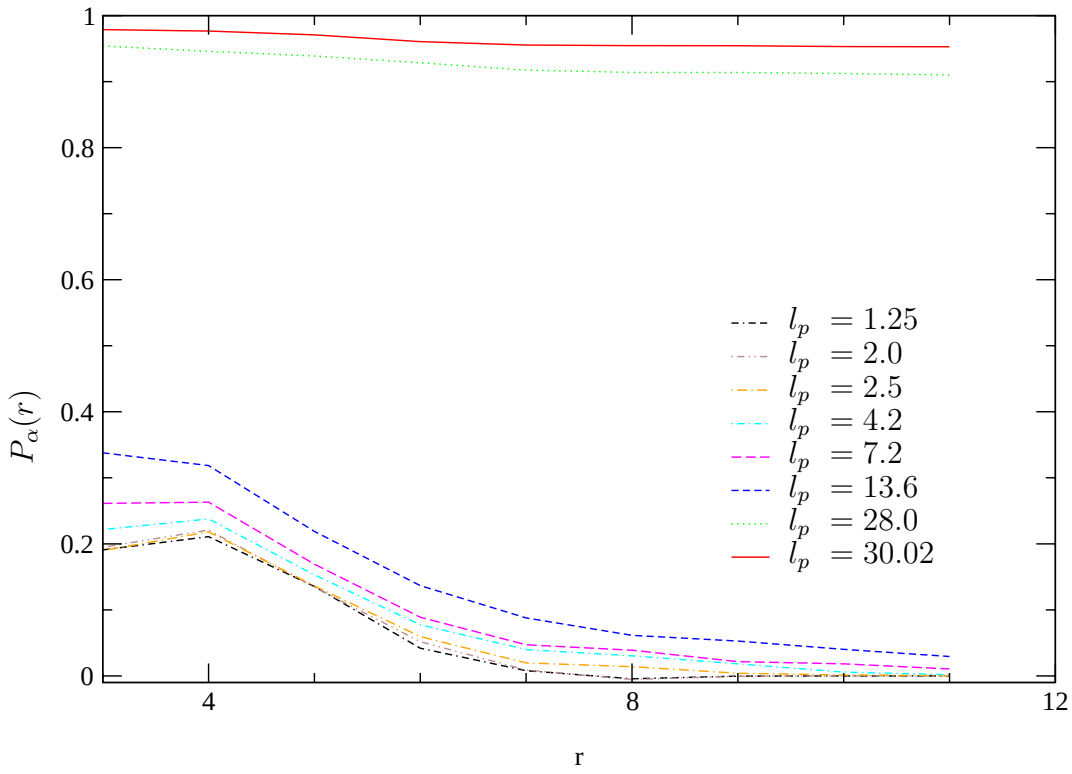

Figure 3.14: Orientational correlation between two bonds of different chains. Long range orientational order is obtained for $\frac{l_p}{a} > 13.6$. Above shown persistence lengths (l_ps) are in unit of average bond length (a).

Additionally, single chain orientational parameters introduced above, the orientational correlation between bond vectors of different chains is of interest. The orientational correlation, ($P_\alpha(r)$), between bonds from different chains is defined by the following way.

$$P_\alpha(r) = \frac{3 < \cos^2(\alpha) > -1}{2} \tag{3.12}$$

where α is the angle between bonds of different chains separated by a distance r. In the case of **nematic ordering** (when all the bonds in different chains are parallel), $P_\alpha(r) = 1$. In a complete uncorrelated case there is no orientational correlation between two different bonds and hence $P_\alpha(r) = 0$. When the bonds in different chains are perpendicular, $P_\alpha(r) = -0.5$. In the intermediate case (i.e. the case between nematic ordering and orientational disorder) $P_\alpha(r)$ lies between 0 and 1. Figure 3.14 shows the profile of $P_\alpha(r)$ for all the stiffness disparity systems studied in the present work. From figure 3.14, it is observed that there is no nematic ordering in our systems of study upto the persistence length ($\frac{l_p}{a}$) of the semiflexible component 13.6 which is consistent with

the nematic order parameter calculated in the previous sub-subsection. As we expect the value of the orientation correlation increases when the stiffness of the semiflexible component increases.

3.3 Model for Monomer Size Disparity

In the previous section, the model for stiffness disparity was discussed. In this section the model for monomer size disparity will be discussed.

3.3.1 Model

We performed again computer simulations of a sandwich type two-component system of homopolymers with different monomer sizes. Figure 3.15 shows a typical snapshot of such a system. The coarse grained continuous space model is used, similar to the cas of stiffness disparity. In these systems, there are two types of monomers; type A having diameter $d_A = d_{min} = \sqrt{3}$, as in the case of stiffness disparity systems, and type B having diameter $d_B = 2 \times d_A$. These systems in general are known as "systems with monomer size disparity". The following types of dispair systems are studied;
(a) $d_B = 2 \times d_A$ and $N_A = N_B$ i.e. diameter of monomers of type B is double than that of type A and number of monomers per chain in type A chains is equal to number of monomers per chain in type B chains. Such a system is referred as **"monomer size disparity with equal number of monomers per chain"**.
(b) $d_B = 2 \times d_A$ and $R_g^A \sim R_g^B$ ($N_B = \frac{3}{4}N_A$) i.e. diameter of monomers of type B is double than that of type A monomers and radius of gyration of type A chains is almost equal to that of type B chains which is referred as **"monomer size disparity with almost equal radius of gyration"**.

The interfacial properties of above two kinds of systems are compared to that of the symmetrical system in which two types of monomers differ only by their interaction. The symmetrical system is same as flexible-flexible polymer system in the case of stiffness disparity case.

The polymer chains are modeled by a succession of jointed spherical monomers according to rod-bead model [42, 7], same model as in stiffness disparity case. A chain consists of N spheres of equal diameter which are connected by (N-1) bonds. For A types of chains we consider N =32. However, for B types of chains there are two cases to study two different kinds of systems (a) and (b) as described above. In the system of monomer size disparity with equal number of monomers per chain, each type B chain has N = 32 monomers whereas in the system of monomer size disparity with almost equal radius of gyration, each type B chain consists of N =24 monomers.

Since there are two types of monomers with different sizes, the excluded volume also depends upon the types of monomers and it is given by the following potential;

$$V_{BB,ex}(r) = \begin{cases} 0 & , \text{ if } r > d_B \text{ (diameter of type B monomers)} \\ \infty & , \text{ else} \end{cases}$$

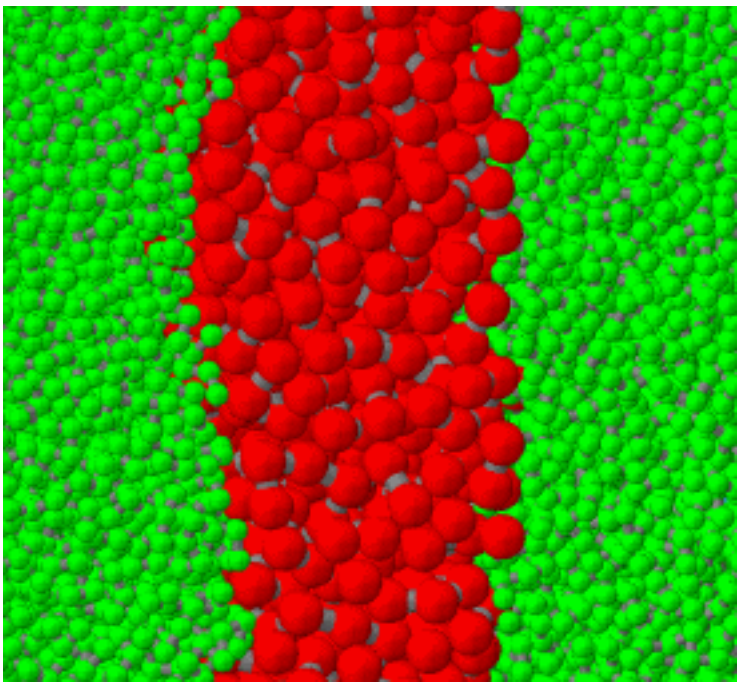

Figure 3.15: A typical snapshot of a monomer size disparity system. Monomers from Red chains have diameter double than that of monomers from green chains.

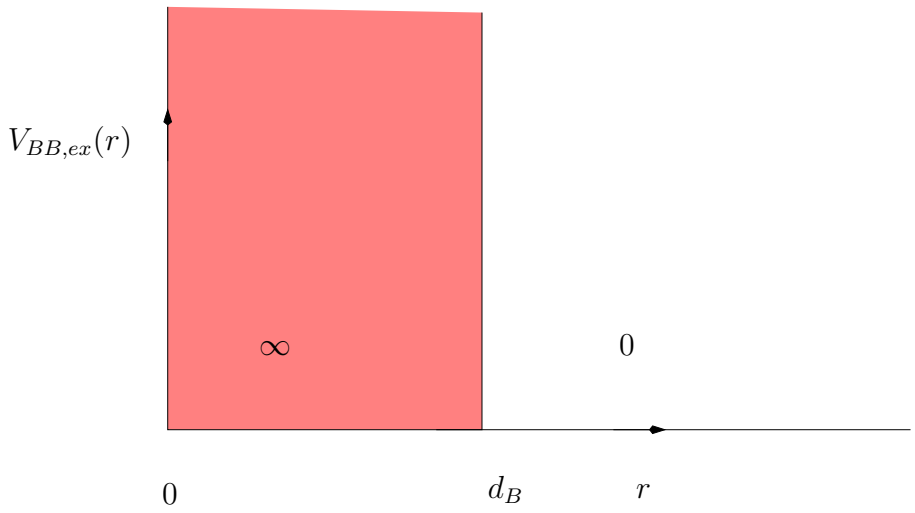

Figure 3.16: Excluded volume potential between two type B monomers in monomer size disparity systems.

where $V_{BB,ex}(r)$ is the excluded volume potential between two type B monomers at a distance r. This excluded volume potential is shown in the figure 3.16.

Similarly, the excluded volume potential between type A and type B monomers is given by;

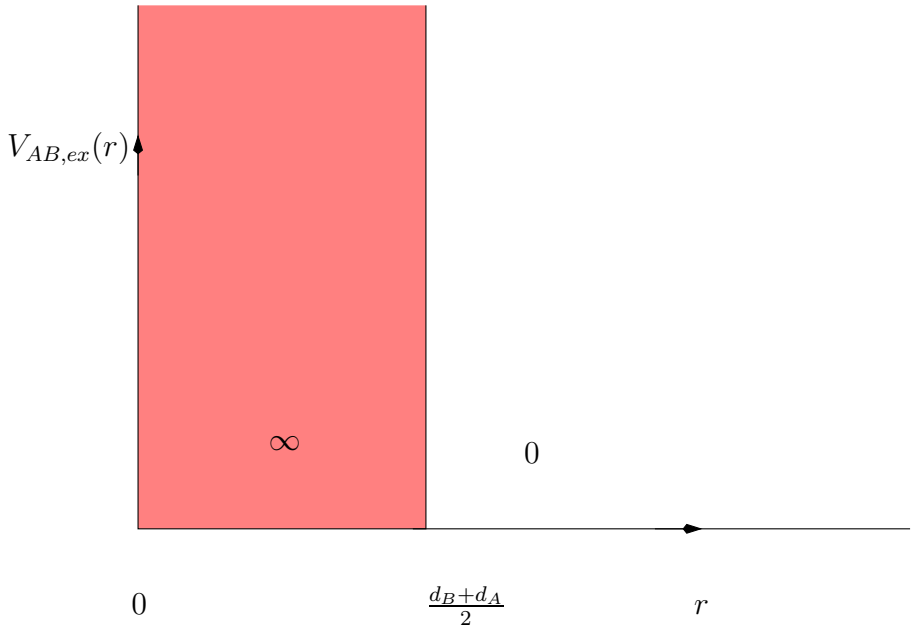

Figure 3.17: Excluded volume potential between type A and type B monomers in monomer size disparity systems.

$$V_{AB,ex}(r) = \begin{cases} 0 & , \text{ if } r > \frac{d_B+d_A}{2} \\ \infty & , \text{ else} \end{cases}$$

where $\frac{d_B+d_A}{2}$ is the minimum distance between type A and type B monomers and $V_{AB,ex}(r)$ is the excluded volume potential between type A and type B monomers at a distance r. $V_{AB,ex}(r)$ is shown in the figure 3.17. The excluded volume potential between any type A beads is same as the excluded volume potential between two beads in stiffness disparity case as discussed in subsection 3.2.1 (see Eq. 3.1 and figure 3.2). Similarly, the connectivity between two consecutive monomers in a type B chains is assured by the following potential;

$$V_{con,B}(r) = \begin{cases} 0 & , \text{ if } d_B \leq r \leq d_{Bmax} \\ \infty & , \text{ else} \end{cases}$$

where $d_{Bmax} \sim \frac{7}{3} d_{min}$, $V_{con,B}(r)$ is the connectivity potential between two consecutive beads of a type B chain separated by a distance r. This value of d_{Bmax} ensures that there is not intersection between type A and type B chains. $V_{con,B}(r)$ is shown in the figure 3.18. The potential for the connectivity of two consecutive monomers from type A chains is same as that in the case of stiffness diaparity, discussed in subsection 3.2.1. Therefore, the distance between any two consecutive beads of a chain depend upon whether the spheres are type A or type B.

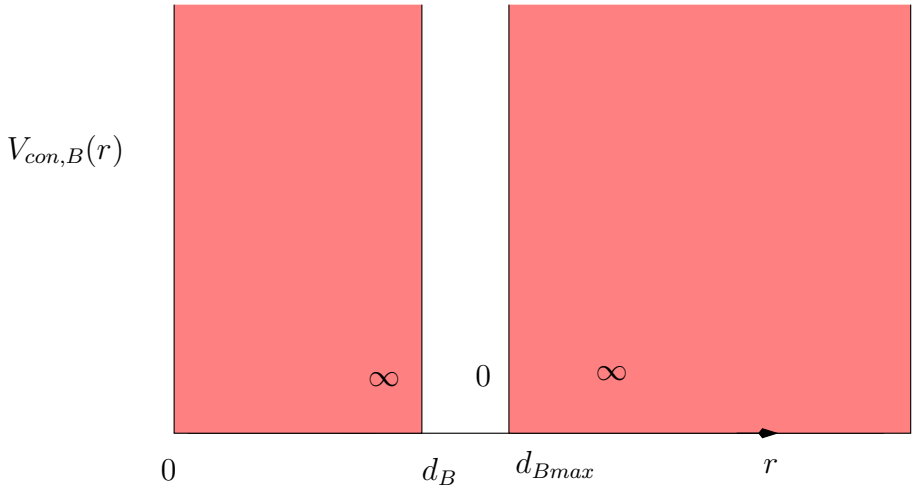

Figure 3.18: Conectivity potential between two consecutive monomers from type B chains in monomer size disparity systems.

The interaction between segments which are not directly jointed is also modeled by a stepwise potential. For simplicity we assume that the interaction between equal types of monomers A and B, $V_{AA} = V_{BB} = 0$ and a repulsive potential acts between different types of monomers $V_{AB,int} = k_B T\varepsilon$ where k_B is the Boltzmann constant, T is the temperature and ϵ is a parameter to be chosen in the model which defines the Flory-Huggins parameter χ and $\epsilon = 0.1$, in the present work. The assumed range of the interaction between two different types of monomers is $d1_{2type} \sim \left(\frac{1}{2} + \sqrt{\frac{5}{3}}\right) d_{min}$. Therefore, the interaction potential between two different types of monomers is given by the following potential;

$$V_{AB,int}(r) = \begin{cases} k_B T\varepsilon & , \text{ if } \frac{d_B+d_A}{2} \leq r \leq d1_{2type} \\ 0 & , \text{ if } r > d1_{2type} \\ \infty & , \text{ if } r < \frac{d_B+d_A}{2} \end{cases}$$

where $V_{AB,int}(r)$ is the interaction potential between type A and type B monomers separeted by a distance r. As mentioned above, the interaction parameter ϵ is related to the Flory-Huggins parameter χ which is estimated in our model in the following way;

$$\chi = z_{eff}\varepsilon \tag{3.13}$$

where z_{eff} is the average number of interchain contacts of a monomer within a sphere of radius of the interaction range between type A and type B monomers in an athermal mixture of two types of chains (see Fig 3.20). From table 3.2 it can be seen that χ decreases for the unsymmetric systems (that is system with different sizes of monomers) as z_{eff} decreases for such systems.

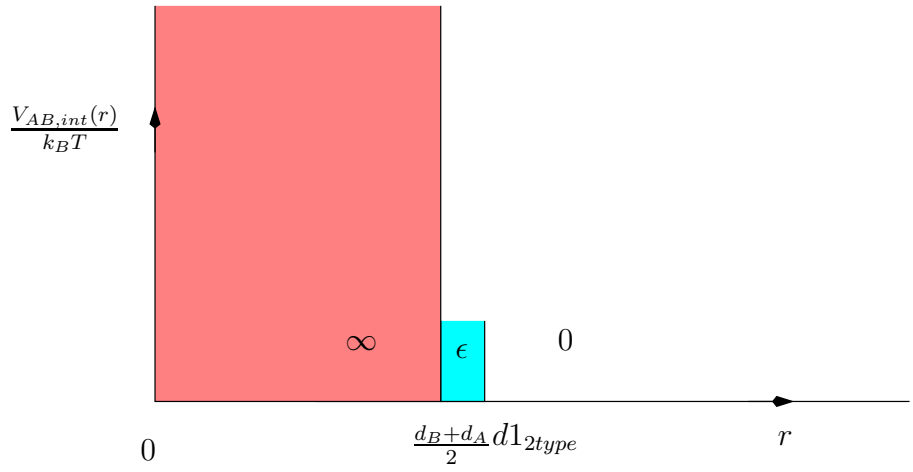

Figure 3.19: Interaction potential between type A and type B monomers separated by a distance r in the monomer size disparity systems.

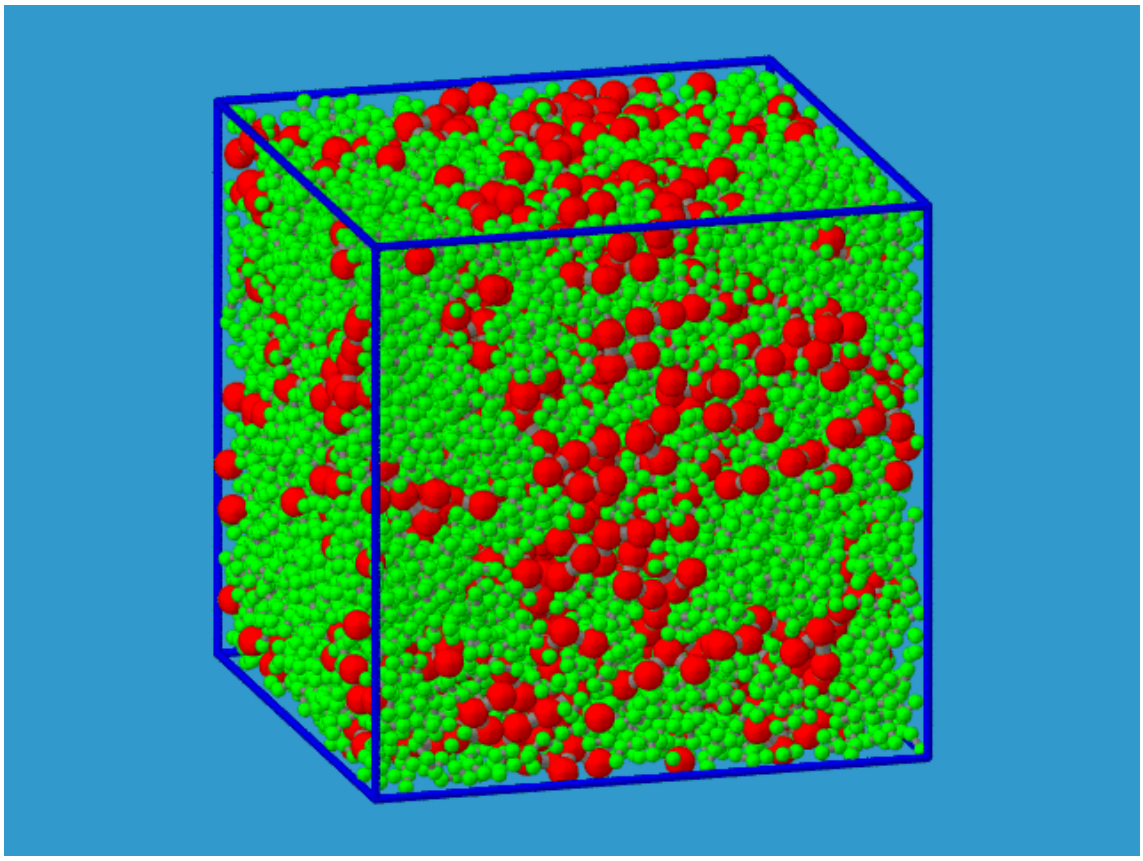

Figure 3.20: Povray diagram of an athermal mixture of monomer size disparity system with equal number of monomers per chain.

3.3.2 Generation of Chains, Equilibration and Single Chain Properties

Generation of chains

To generate the system of monomer size disparity with equal number of monomers per chain, 32 random walk chains (type A chains) with random bond length distribution $d_{min} \leq d \leq d_{max}$ with no overlap with next nearest neighbors within the chain [47] are generated. Other four random walk chains (type B) are generated with random bond length distribution $d_B \leq d \leq d_{Bmax}$ with no overlap with next nearest neighbors within the chain. Each chain consists of 32 monomers per chain. To generate the size disparity system with almost equal radius of gyration, 6 random walk chains (type B chains, each chain having 24 monomers per chain) with random bond length distribution $d_B \leq d \leq d_{Bmax}$ with no overlap with next nearest neighbors within the chain are generated. The type A chains are generated following the same way as described above and there are 32 type A chains in both the systems. The symmetric system is same as the system of only flexible chains in the stiffness disparity case.

To generate the interface initially, a box having three compartments in which the middle one has volume double than that of both sides (this simulation box has dimensions- $64 \times 16 \times 16$) is considered. One fourth of both sides of the box (across x-dimension) occupy type A chains and the remaining half of the lattice in the middle with type B chains. The overlaps between the segments is removed by stepwise increase ("blowing up") of the diameter of the spherical monomers followed by Monte-Carlo steps. This process is started with the minimum distance of any monomers which are not directly connected. For symmetric system, the process lasts when the minimum distance between any two monomers is equal or greater than d_{min}. However, for unsymmetric systems, the process goes on until the distance between any two type B monomers is equal or greater than d_B, the distance between any two type A monomers is equal or greater than d_{min} and distance between type A and type B monomers is equal or greater than $\frac{d_B+d_A}{2}$. The system is enlarged by shifting y and z coordinates to get a system having dimensions $64 \times 32 \times 32$ - parallelepiped. In doing so number of chains is increased by four times. We further multiply the system by shifting y and z coordinates to get final system of study $64 \times 64 \times 64$ -cube. The final system consists of 512 type A chains and 64 type B chains in the system of monomer size dispartiy with equal number of monomers per chain. Similarly, it has 512 type A chains and 96 type B chains in the system of monomer size dispartiy with almost equal radius of gyration. Figure 3.21 shows an initial configuration for the system of monomer size disparity with equal number of monomers per chain.

Equilibration of chains

For equilibration and thermodynamical averaging the Monte-Carlo steps have been performed according to the standard Metropolis algorithm with random choice of a monomer and cyclic choice of one of the six directions along the coordinate axes, as

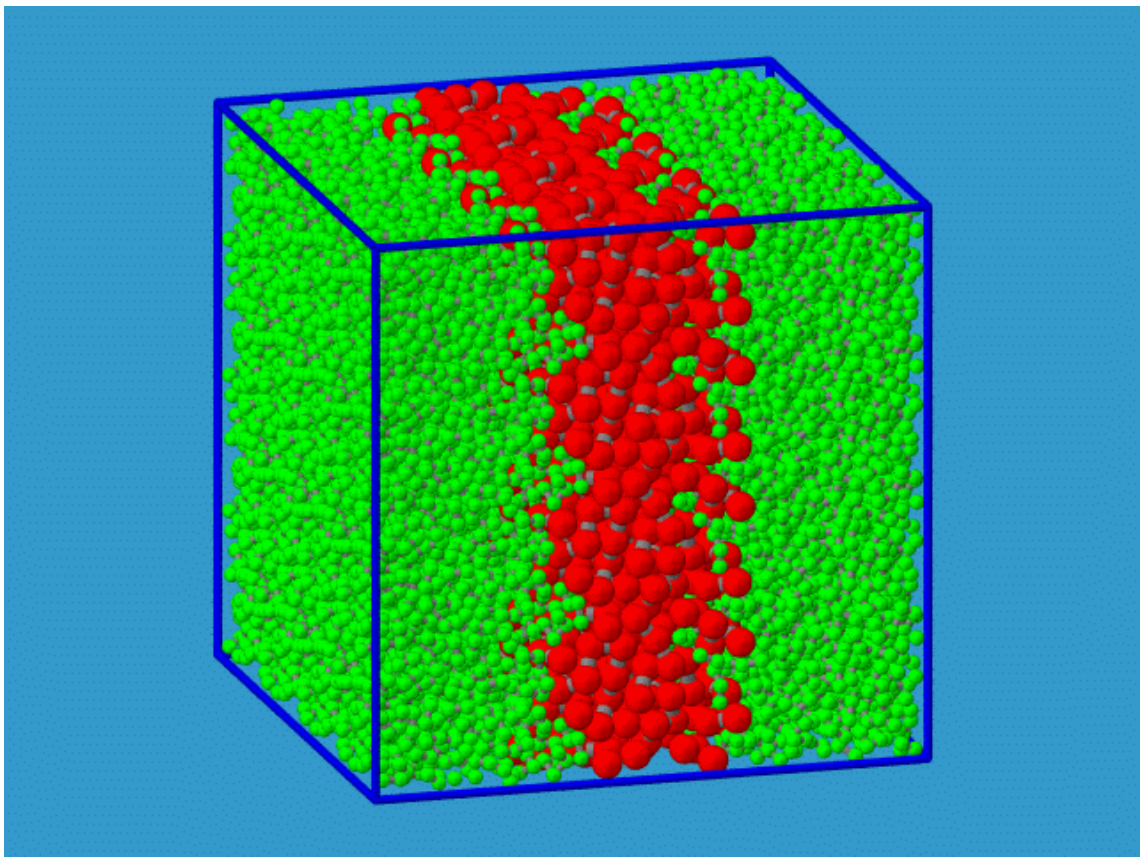

Figure 3.21: Povray diagram of initial configuration of monomer size disparity with equal number of monomers per chain.

described in the stiffness disparity system. The length of an attempted step is chosen randomely between zero and a maximum step length $\sim\ 0.23 \times d_{min}$. To accelerate the tests for hard-core overlapping and for the calculations of the interaction energy after each attempted move, we follow the standard way by dividing the simulation box into cubic cells of size l_c with single occupancy for type B monomers and checking the particles in the neighborhood of the moved particle only. There could be several particles of type A monomers in a cubic cell. Therefore, in this case we have to check overlapping of moved particle within cell also (see the flow diagrams 3.25, 3.26). For the symmetric system, we consider a cubic cell of size unity, so that there will be only single occupancy for type A and type B monomers. The techniques of equilibration of chains for the stiffness disparity systems and size disparity systems differ in the following way. **In the former case, in linked cell method we chose the size of cell such that there is single occupancy for both types of monomers and in the later case, the size of a cell is such that larger size of beads occupy single cell and hence there could be many monomers of type A in the same cell**. The details of the linked cell method are described by Allen and Tildesley and by Sadus [77, 78]. Auhl

[7] has already applied the linked cell method for the flexible-flexible polymer systems. If there are many particles in one cell, during sorting of particles in appropriate cells two arrays are created namely, 'head-of-chain' (HEAD) and 'linked-list' (LIST). HEAD has one element for each cell and it contains the identification number of one of the particles sorted into that cell. This number is used to address the element of a LIST, which contains the number of the next particle in that cell. In turn, the LIST array element for that particle is the index of the next particle in the cell, and so on. By following the trial of link-list references, we will eventually reach an element of LIST which is zero. This indicates that there are no more particles in that cell, and we move on to the HEAD particle for the next cell and so on. Two well defined interfaces are enforced in the canonical ensemble in a thick film geometry ($L \times L \times L$), with periodic boundary conditions in all the three directions. The interfaces are on average located in $\frac{1}{4}$th and $\frac{3}{4}$th of the x-dimensions of the simulation box.

To know whether systems have attained equilibrium configurations, the same idea like in the case of stiffness disparity, is followed. The parallel and the perpendicular (parallel and perpendicular according to the interface) components of the radius of gyration, R_g, and the mean squared displacement of center of mass of chains (ΔMSD) against the simulation time are monitored. The figure 3.22 presents (ΔMSD) of center of mass of chains and mean squared parallel and perpendicular components of radius of gyration for the system in which two types of monomers have different sizes but equal number of monomers per chain. For each system of study, the ΔMSD of center of mass of chains and parallel and perpendicular components of R_g^2 are monitored and until both of these are comparable we do not start calculation of interfacial tension and other quantities. The ΔMSD of individual components are also not significantly different than that of total system. Further the values of interfacial tensions after the calculations are also monitored. The values of interfacial tensions of the system, in which both types of chains have equal number of monomers per chain but different sizes of monomers, against number of measurements are depicted in figure 3.23. They also show that (as the values do not change monotonically with the time of measurements) the systems are close enough to equilibrium at the time of measurement. To get equilibrium state we performed 6.1×10^5 attempted moves per monomer (AMM) for the symmetric system, i.e. the system with the same sizes of monomers. However, for the system having different sizes of monomers we have to perform 10^7 AMM. Figure 3.24 depicts an equilibrium system in which both types of chains have equal number of monomers per chain but two types of monomers have different sizes.

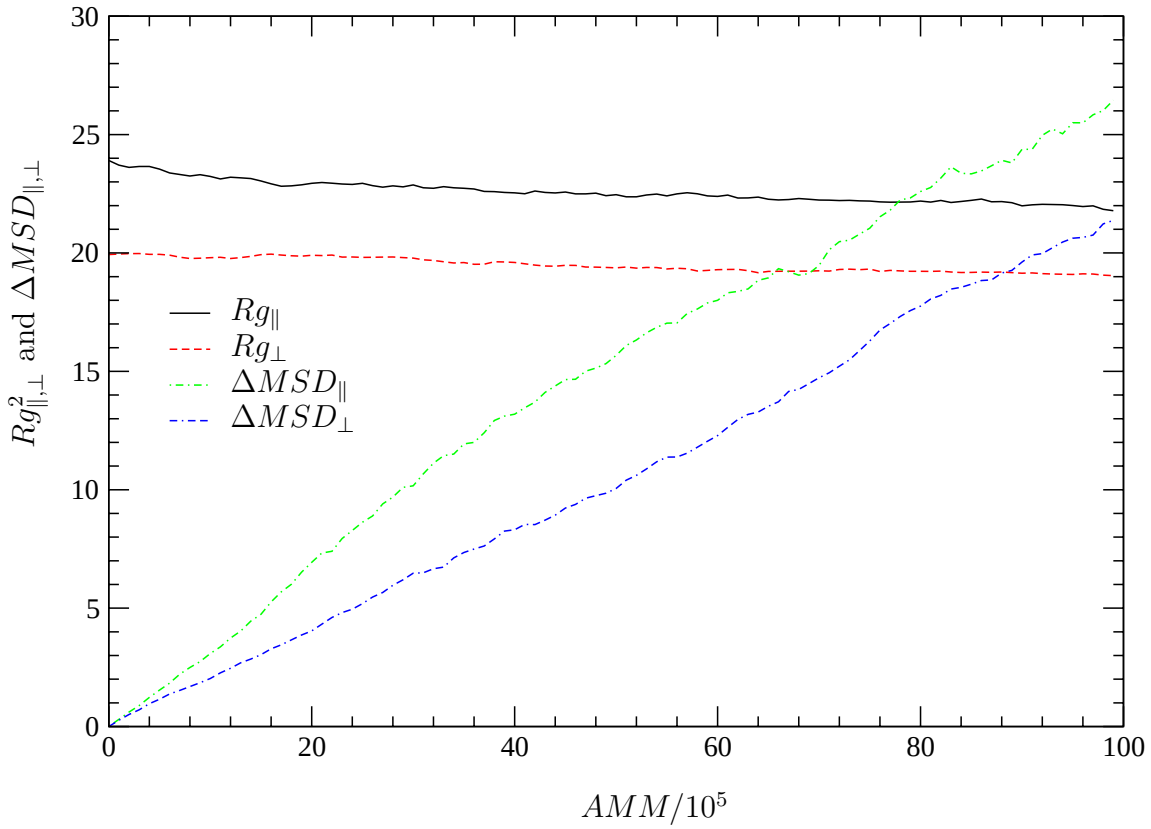

Figure 3.22: Perpendicular and parallel components of square of radius of gyration and mean squared displacements of center of mass for the system with monomer size disparity with equal number of monomers per chain.

Single Chain Properties

The single chain conformations are presented in table 3.2 (page 37). When the diameter of type B monomers is larger than that of type A monomers the ratio $\frac{R^2}{R_g^2}$ will be higher than 6. The dependence of $\frac{R^2}{R_g^2}$ on segment number of the B type of chains shows that type B chains are slightly stiff. Here also the statistical segment length b is defined according to equation 3.4. The statistical segment length for the type B chains with 24 monomers per chain is determined according to equation 3.4 using C_{1N} for $N = 32$. In table 3.2, R^2 is the mean squared end to end distance, R_g^2 is the mean squared radius of gyration, b is the statistical segment length and χ is the Flory-Huggins parameter, N is number of monomers per chain and N_P is the number of chains in the system of study.

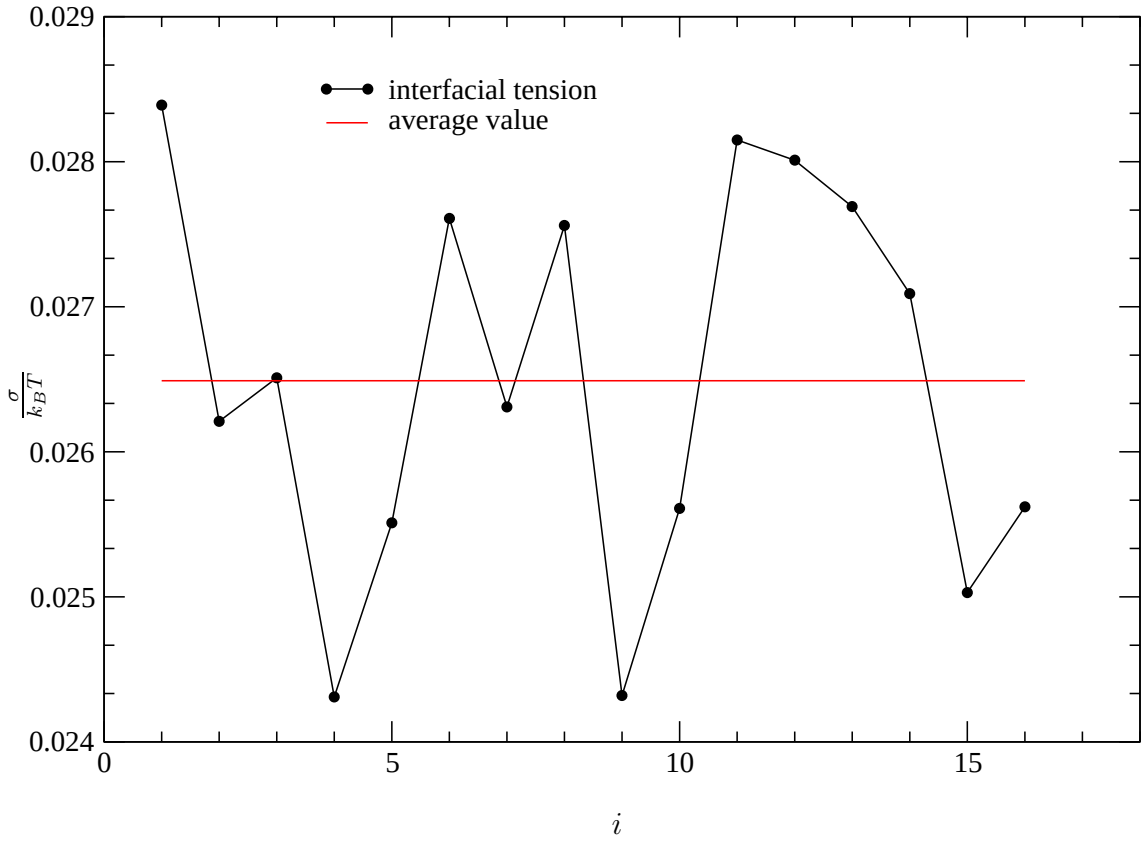

Figure 3.23: Interfacial tension versus number of calculations for the system with monomer size disparity with equal number of monomers per chain. There are 4.8×10^4 AMM between two successive calculations.

3.4 Calculation of the Interfacial Tension

In the present systems of study, due to different kinds of disparities, i.e. the stiffness disparity in the flexible-semiflexible blend and monomer size disparity in monomer size disparity systems, a straight forward application of the semi-grand-canonical identity changes between different polymer types are rather inefficient. Therefore, the interfacial tension cannot be calculated by the reweighting of the composition distribution as successfully applied in most Monte Carlo investigations interfacial tension [29]. Alternatively, we can calculate the interfacial tension by analyzing the spectrum of the capillary fluctuations and as advantage of off-lattice model by using virial theorem. The virial theorem method successfully applied to determine the free energy costs of a hard wall [74] in a concentrated polymer solution, and to determine the interfacial tension [7, 73] in a binary polymer blend. Auhl [7] has calculated anisotropy in the pressure tensor in flexible-flexible polymer systems for the same chain model as in present study. In the present work the method used by Auhl, is extended to apply for the flexible-semiflexible polymer systems and a system containing polymers with different monomer sizes.

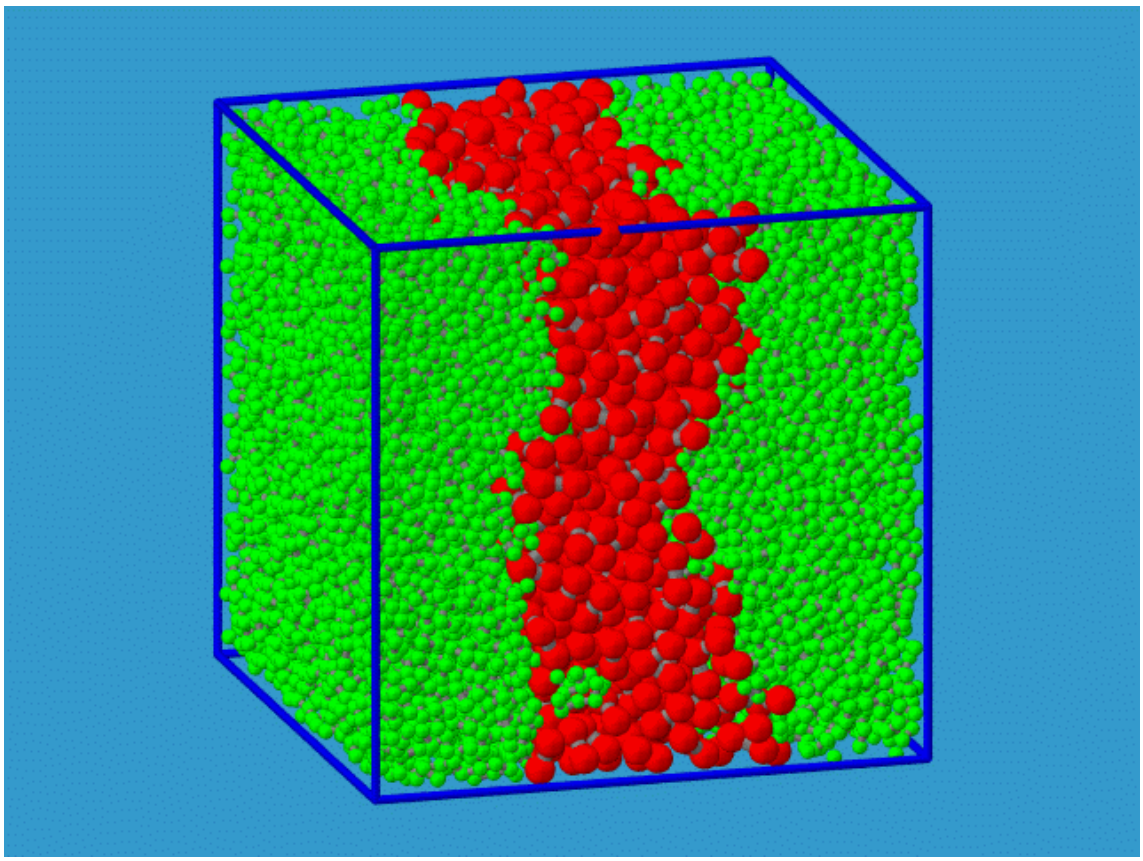

Figure 3.24: Povray diagram of final configuration of monomer size disparity system with equal number of monomers in a chain.

Virial theorem method

Calculating the interfacial tension by using virial theorem [77] is one of the most direct and rigorous methods, it rests on the determination of the anisotropy of the pressure tensor of a system with an interface.

The interfacial tension, σ can be expressed as,

$$\frac{\sigma}{k_B T} = \frac{\Delta F}{\Delta A} \tag{3.14}$$

where ΔF is the change in the free energy for a corresponding change ΔA in the cross sectional area, k_B is Boltzmann constant and T is temperature.

The change of free energy can be calculated by considering the forces caused by a small deformation of the simulation box. This results in

$$\frac{\sigma}{k_B T} = \frac{f_\perp L_\perp}{L_\parallel^2} - \frac{f_\parallel}{L_\parallel} \tag{3.15}$$

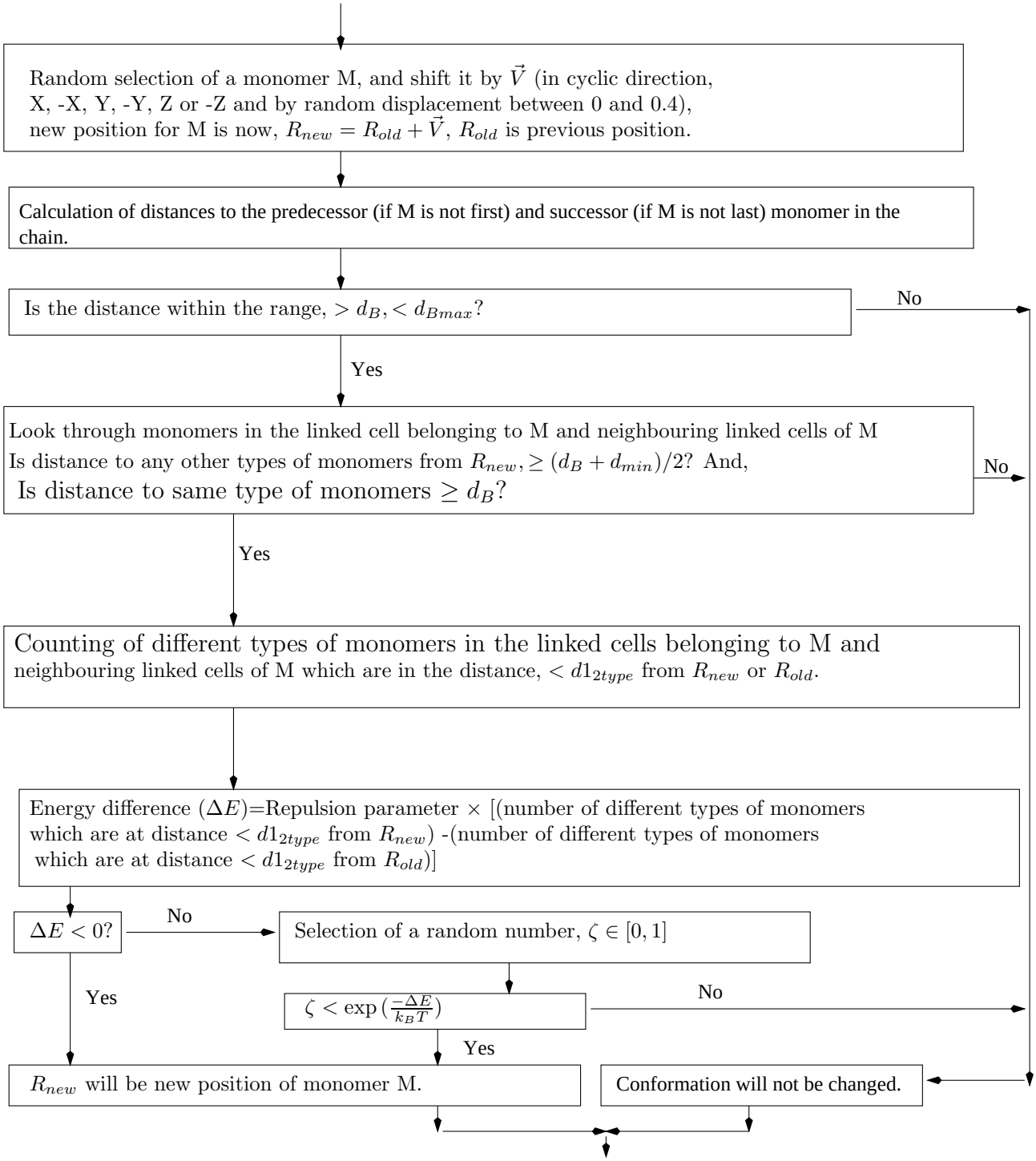

Figure 3.25: Flow diagram for a monomer from type B chains that is, for a larger size monomer.

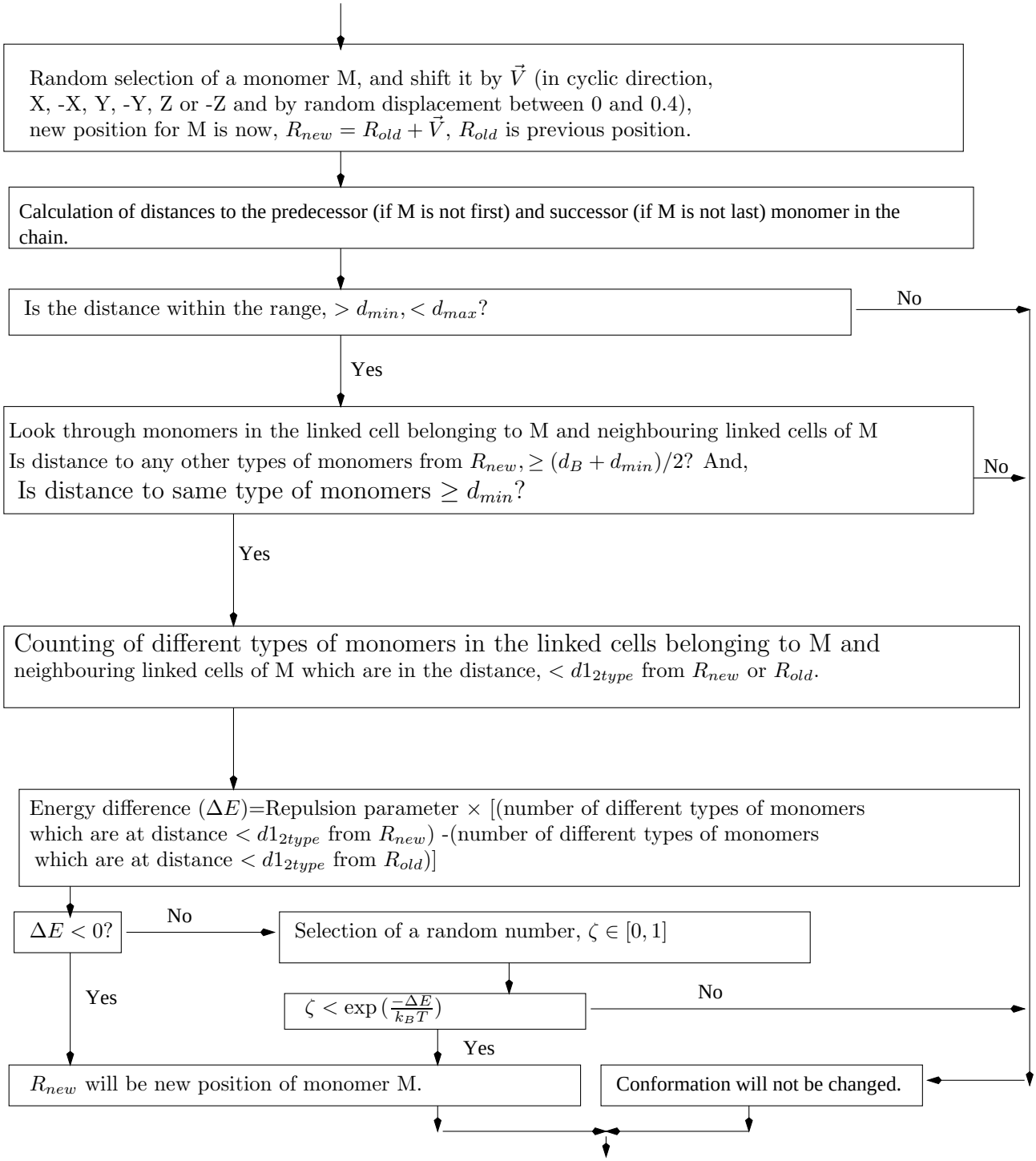

Figure 3.26: Flow diagram for a monomer from type A chains that is, for a smaller size monomer.

type of chains	N	N_P	R^2	R_g^2	$\frac{R^2}{R_g^2}$	$\frac{b}{a}$	χ
A	32	512	193	32	6.03	1.51	0.32
B	32	64	709	112.36	6.31	1.62	0.196
B	24	96	480	64	7.5	1.62	0.212

Table 3.2: Single chain conformations as a function of monomer diameter of chains. In this table statistical segement lengths are in units of average bond length for the respective type of chains. For the chains with smaller bead the average bond length is 1.998 whereas for the chains with larger beads it is 3.749.

where $f_{\perp,\parallel}$ are the forces acting on the boundary of the simulation box perpendicular and parallel with respect to the interface plane. $L_\perp$ is the length of the system perpendicular to the interface plane and $L_\parallel$ is the length of the system parallel to the interface plane. The force is calculated by a small homogeneous uniaxial deformation of the chains. The details of this method is described in [7]. The deformation (which we suppose a small uniaxial compression/expansion of the probe) matrix, we use in our method is given by;

$$\begin{pmatrix} 1+\alpha & 0 & 0 \\ 0 & 1 & 0 \\ 0 & 0 & 1 \end{pmatrix} \tag{3.16}$$

where α is deformation parameter. Using virial theorem the force components $f_{\perp,\parallel}$ can be expressed as [7];

$$\frac{f_{\perp,\parallel}L}{k_BT} = \frac{d}{d\alpha}\bigg|_{\alpha=0} \ln \left\langle \exp\left(-\Delta E(\alpha)/k_BT\right)\right\rangle_0 \tag{3.17}$$

where $\langle(\ldots)\rangle_0$ denotes average of $(\ldots)$ in the undeformed system and $\Delta E(\alpha)$ is the difference in total potential energy of deformed and undeformed conformations. This formula is general and is valid for any models. The differential coefficient in equation 3.17 is not so easy to calculate. Therefore, we calculate the differential coefficient in right hand side of Eq. 3.17 by a set of finite difference quotients. One can write,

$$\frac{d}{d\alpha}\bigg|_{\alpha=\alpha_i} \ln\left\langle \exp\left(\frac{-\Delta E(\alpha)}{k_BT}\right)\right\rangle_0 \approx \frac{\Delta \ln\left\langle \exp\left(\frac{-\Delta E(\alpha)}{k_BT}\right)\right\rangle_0\Big|_{\alpha_i}}{\Delta\alpha} \tag{3.18}$$

for very very small $\Delta\alpha$. To evaluate right hand side of Eq. 3.17, we find a set of such finite differences for several α_i's and extrapolate it to $\alpha = 0$.

In the case of the step potentials, U_i, Eq. 3.18 and hence Eq. 3.17 can be further simplified and finally we get,

$$\frac{f_{\perp,\parallel}L}{k_BT}\bigg|_\alpha = \sum_i \frac{1}{\Delta\alpha}\left\langle \Delta W_i M_i(\alpha, \alpha+\Delta\alpha)\right\rangle_{configurations} \tag{3.19}$$

where i is the type of interaction (there are four types of interaction for semiflexible and three types of interactions for flexible polymer chains),

$$\Delta W_i = 1 - (\exp(-\Delta U_i / k_B T))$$

is the change of weight and

$$M_i(\alpha, \alpha \pm \Delta\alpha)$$

is the number of monomers entering/leaving the interaction range for i of another monomer when changing the compression/expansion from α to

$$\alpha \pm \Delta\alpha.$$

To use the full information contained in a given configuration of chains and to optimize the averaging we consider small $\Delta\alpha$, calculate the force for several α and extrapolate so obtained set $\left.\frac{f_{\perp,\parallel} L}{k_B T}\right|_{\alpha}$ to $\alpha = 0$. For the systems considered in the present work, the contributions to the pressure tensor from all the interactions present have to be calculated. These are the excluded volume, chain connectivity, the repulsing interaction between different types of the monomers and the bending energy (only for the semiflexible chains).

The distance between the monomer pairs in the case of small compression/expansion of the probe will be within interaction neighbourhood ('collisions'), divided by the deformation factor α and multiplied by a weight factor which is derived from the height of the step potential. The potential which models the connectivity in our model will play a role when the distance is larger than certain distance, the potential which models the repulsion between different types of monomers will play the role when the distance is larger/smaller than certain distance. The potential which takes into account excluded volume effect in our model plays a role when the distance between any two monomers is less than the certain distance and the potential which models the bending energy (in semiflexible polymers) in our model will play a role when the angle between two consecutive bond vectors of a chain is greater than a certain angle.

Next, the deformation factor α has to be considered, this depends up on the fact whether compression is considered or expansion. Further it depends up on whether our system is stiffness disparity or monomer size disparity. At the first we describe various weight factors for stiffness disparity systems and then for monomer size disparity systems.

For the four interactions which appear for monomer pairs in heterogeneous polymer models (flexible-semiflexible polymer system) used in present study, one obtains the following weight factor;

- Excluded Volume: $E = 0$, if the distance is $> d_{min}$, ∞, else, between any two monomers and it is applicable just for compression, weight factor 1.

- Connectivity: $E = 0$, if the distance is $< d_{max}$, ∞, else, between any two consecutive monomers in a chain and it is applicable just for expansion, weight factor 1.

- Bending Energy: $E = 0$, if the angle is $> \theta_{max}$, ∞, else, between any two consecutive bond vectors in a semiflexible chain and it is applicable for expansion/compression, weight factor 1.

- Repulsion: Repulsion between different types of monomers; $E = \epsilon$, if distance between two monomers is $< d_{2type}$, $E = 0$, else, and $\epsilon = 0.1$ acts between all the different types of monomers and applicable for compression/expansion with weight factor $(1 - \exp(-\epsilon))$ in the case of compression (in case a monomer falls to the interaction range of the other) and weight factor $\exp(\epsilon) - 1$ in the case of expansion (in case monomer just goes out of the interaction range of the others).

Similarly, for the three interactions which appear for monomer pairs in heterogeneous polymer models (polymer with different sizes of monomers) used in present study, one obtains the following weight factor;

- Excluded Volume: $E = 0$, if the distance between any type B monomers is $> d_B$, ∞, else.
  $E = 0$, if the distance between any type A monomers is $> d_{min}$, ∞, else.
  $E = 0$, if the distance between any different types of monomers is $> \frac{d_B + d_{min}}{2}$, ∞, else, and it is applicable just for compression, weight factor 1.

- Connectivity: $E = 0$, if the distance is $< d_{Bmax}$, ∞, else, between any two consecutive monomers in a type B chain.
  $E = 0$, if the distance is $< d_{max}$, ∞, else, between any two consecutive monomers in a type A chain, and it is applicable just for expansion, weight factor 1.

- Repulsion: Repulsion between different types of monomers; $E = \epsilon$, if distance between two monomers is $< d1_{2type}$, $E = 0$, else, and $\epsilon = 0.1$ acts between all the different types of monomers and applicable for compression/expansion with weight factor $(1 - \exp(-\epsilon))$ in the case of compression (in case a monomer falls to the interaction range of the other) and weight factor $\exp(\epsilon) - 1$ in the case of expansion (in case monomer just goes out of the interaction range of the others).

Capillary wave spectrum method

An alternative way of measuring the interfacial tension is the analysis of the capillary fluctuation spectrum [38, 73, 81, 82]. In general, polymer-polymer interfaces are not flat but exhibit long-wavelength capillary wave fluctuations. In the case of interface, there exits a type of fluctuation that survives even deep in the two-phase region. This is

because the interface breaks a continuous symmetry, the translational invariance, which results existence of long-wavelength transversal excitations known as Goldostone bosons [81]. The energy of these capillary waves of the local interface position vanishes as the wave length approaches infinity. These fluctuations strongly influence all quantities that depend on transversal degrees of freedom [81]. Capillary wave-like distortions of the interface can be thermally driven even at low temperatures because they cost very little energy. The effects of such fluctuations on interfacial properties were first considered by Buff *et al.* [83] and later systematically studied by Werner *et al.* [81, 84] and Lacasse *et al.* [73]. Capillary wave distortions can occur at large wave length with very little energy cost and are ultimately suppressed by finite size effects (system boundaries). The thermally excited capillary waves will be present at a polymer-polymer interface, even far away from the critical point, and such capillary waves may make a significant contribution to the measured interfacial width [85]. Moreover, the apparent width of a capillary-wave-roughend interface will depend on the length scale over which the interface will be averaged by the measurement (see figure 3.4) which will differ according to the technique used.

Let the deviation of the interfacial position from its mean position be $h(y, z)$. According to the capillary wave theory [84] the free energy cost of these fluctuations is proportional to the increase in the interfacial area caused by these fluctuations. Hence, the free energy cost for the deviations from a flat planar interface is given by [84]

$$H_{cw} = \int \frac{\sigma}{2} (\nabla h)^2 \; dz \; dy + ... \tag{3.20}$$

In this expression, higher order gradient terms are assumed to be very small and neglected. σ is the interfacial tension. This capillary wave hamiltonian can be diagonalized by means of the Fourier transformation with respect to y and z which yields,

$$H_{cw} = \frac{\sigma}{2} \sum (\vec{q}^2) |h(\vec{q})|^2 \tag{3.21}$$

where $\vec{q}$ is the wave vector. From the equipartition theorem one can easily get the mean squared value of $h(\vec{q})$) which is,

$$< |h(\vec{q})|^2 >= \frac{1}{(\sigma \vec{q}^2)} \tag{3.22}$$

Therefore, the local mean squared displacement of the interface is given by,

$$s^2 = \sum_{\vec{q}} \left\langle |h(\vec{q})|^2 \right\rangle = \frac{1}{4\pi^2} \int \left\langle |h(\vec{q})|^2 \right\rangle \; dq = \frac{1}{2\pi\sigma} \ln \left(\frac{q_{max}}{q_{min}} \right) \tag{3.23}$$

Here the lower cut-off q_{min} and the upper cut-off q_{max} have to be introduced as the integral $\int \frac{dq}{q}$ diverges logarithmically both for $q \to 0$ and $q \to \infty$. It could be necessary to cut off these divergences in a smooth way, using suitable correction terms in the capillary wave hamiltonian to get the more accurate description [86]. The maximum value of the

wave-vector clearly has to be set by a microscopic distance; it does not make sense to talk about a capillary wave whose wave length is much smaller than the intrinsic diffuseness of the interface, so this sets the value of q_{max}. The wave length cannot be bigger than the total size of the interface, so we are left with conclusion that the roughness of polymer-polymer interface depends on the size of the container. Therefore, the possible minimum value of q is $\frac{2\pi}{L}$ and the maximum value of q is $\frac{2\pi}{B_0}$ where L is the system size and B_0 is the coarse graining length on which the interface assumes its 'intrinsic' structure [81].

In principle, one can find the interfacial tension using capillary wave spectrum method by calculating the local mean squared displacement of the interface i.e. by using the formula 3.23 [81]. However, for this purpose the system should be very large and in the present system of study it cannot be applied. Therefore, in the present work the method used by Lacasse *et al.* [73] and by Auhl [7] is followed.

To find the total interfacial width which contains the effects of capillary wave fluctuations, it is assumed that the capillary waves can be decoupled from fluctuations in density and in order parameter. Hence, the averaged interfacial profile $\Psi(x)$ can be written as the convolution of the intrinsic interfacial profile $\psi(x - x_0)$ and the probability $p(x_0)dx_0$ of finding the interface at x_0 [73],

$$\Psi(x) = \int_{-\infty}^{\infty} \psi(x - x_0)p(x_0)\ dx_0 \tag{3.24}$$

Differentiating with respect to x one gets that $\Psi'(x)$ is the convolution of two well-bounded functions, $\psi'(x - x_0)$ and $p(x_0)$. Associating a functional measure to the well bounded function and using convolution theorem one gets,

$$\Delta^2 = \Delta_0^2 + < (\Delta X_0)^2 > \tag{3.25}$$

where Δ^2 and Δ_0^2 are related to the total and intrinsic interfacial width respectively (see below) and $< (\Delta X_0)^2 >$ is the mean squared fluctuation on the interfacial position at x_0.

Assuming equipartition of thermal energy on the modes of capillary waves and taking into account that a lower cutoff of wave vectors of capillary waves is given by the size L_s of the subsystem considered and a upper cutoff is determined by a scale l_0 of local bending rigidity or the intrinsic width of the interface, for $\langle (\Delta X_0)^2 \rangle$ results [85],

$$\left\langle (\Delta X_0)^2 \right\rangle = \frac{k_B T}{2\pi\sigma} \ln(\frac{L_s}{l_0}) \tag{3.26}$$

and we get finally

$$\Delta^2 = \Delta_0^2 + \frac{k_B T}{2\pi\sigma} \ln(\frac{L_s}{l_0}) \tag{3.27}$$

Determining the effective interface width for a set of subsystems of size L_s the interfacial tension can be determined without assumptions about the lower cutoff l_0. For

this purpose the density profile of the interface within a subbox of cylindrical shape was described by

$$\Psi(x - x_0) = 0.5 \left(1 + \tanh \frac{(x - x_0)}{w} \right) \tag{3.28}$$

and using the relationship $\Delta^2 = (\pi^2/12) \cdot w^2$ from the slope of the dependence of Δ^2 on $\ln(L_s)$ the interfacial tension is obtained by a least square fit. Fig. 3.4 shows the graph of square of interfacial width versus the system size and the least square fitted line for one of the configurations used for the analysis of the capillary wave spectrum.

In the Eq. 3.27, l_0 is the lower cutoff length which is the coarse graining length on which the interface assumes its 'intrinsic' structure [81]. To determine the intrinsic width, we choose persistence length, l_p, of the semiflexible chains as the lower cutoff length. The results obtained in this way will be discussed below.

Using both methods (analysis of capillary wave spectrum and virial theorem) described above, the interfacial tensions from 16 different configurations, such that output of former is input of successive, for each system of study have been calculated in stiffness disparity systems. We performed 2.4×10^4 attempted move per monomer (AMM) between two successive configurations for the systems of flexible chains and number of AMM increased with increasing stiffness of the semiflexible chains. For the system with the highest stiffness of our study the number of AMM between two successive configurations was 6.0×10^4. Fig. 3.12 shows for a system with intermediate stiffness disparity ($\frac{l_p}{a}$ =2.5) the values obtained by both methods for the 16 configurations used for the measurement of interfacial tension. For the size disparity system, the interfacial tension is calculated just by using virial theorem from 16 different configuration such that output of former is input of successive. 4.8×10^4 AMM between two successive configurations were performed. Figure 3.23 shows the interfacial tension from 16 different configurations for the system of monomer size disparity with equal number of monomers per chain. Capillary wave spectrum method could not be used to calculate the interfacial tension for monomer size disparity systems because of small system sizes considered in the present work.

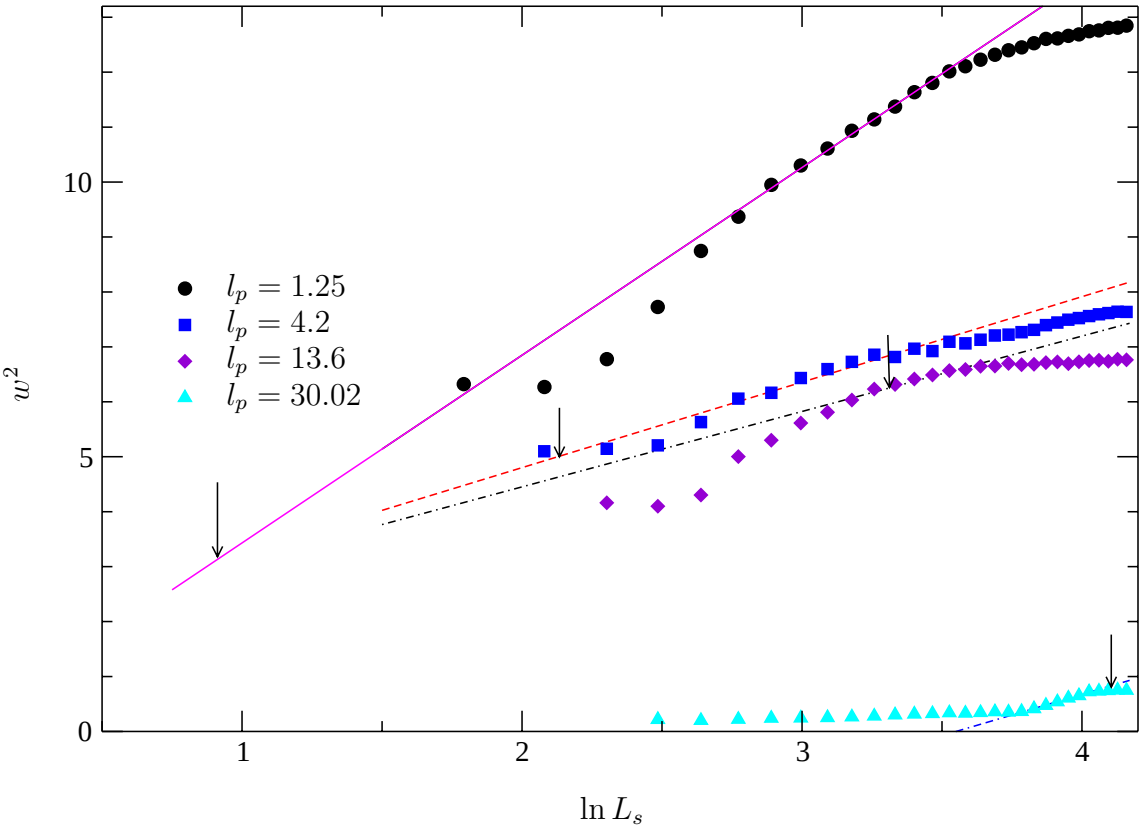

Figure 3.27: Square of interfacial width versus the logarithm of subsystem size, (L_s), as a function of stiffness of the semiflexible components. Arrows mark the square of intrinsic width for the respective systems.